# Simplified geostatistical analysis of earthquake-induced ground response at the Wildlife Site, California, U.S.A

**Tamer Elkateb, Rick Chalaturnyk, and Peter K. Robertson**

**Abstract:** Almost all natural soils are highly variable and rarely homogeneous. In this study, the seismic response of the Wildlife Site, Imperial Valley, California, U.S.A., has been analysed to assess the effect of ground heterogeneity on liquefaction assessment in a probabilistic analysis framework. Cone penetration test (CPT) data recorded at the site have been used to identify different lithologies and to estimate elements of soil inherent spatial variability. Monte Carlo simulation has been utilized to obtain several realizations of CPT data that were then implemented into empirical approaches to examine the liquefaction susceptibility of the site. In addition, stochastic analysis of liquefaction-induced surface damage has been carried out through the application of these realizations into damage criteria, such as total liquefaction damage potential and surface settlement. These stochastic analyses have indicated that using mean values in deterministic analysis can be on the unsafe side. As a result, attempts have been made to obtain meaningful representative soil parameters that can be used in simplified deterministic analysis, while continuing to honor detailed ground heterogeneity. In addition, an empirical technique has been developed to compare ground variability of potentially liquefiable sites on a qualitative basis.

*Key words*: liquefaction, spatial variability, stochastic analysis, cone penetration test, damage, characteristic parameters.

**Résumé** :

*Mots clés* :

[Traduit par la Rédaction]

## Introduction

Seismically-induced liquefaction can be defined as the loss of shear strength and degradation in soil stiffness due to earthquake-induced pore pressure development, up to the value of the total geostatic stresses. Surface evidence of liquefaction can be manifested as ground settlement, lateral spread, sand boils, or extension cracks and may cause damage to overlying structures. Almost all natural soils are highly variable in their properties and are rarely homogeneous. Soil heterogeneity can be classified into two main categories. The first is lithological heterogeneity, which can be manifested in the form of thin soft–stiff layers embedded in a stiffer–softer media or the inclusion of pockets of different lithology within a more uniform soil mass. The second source of heterogeneity can be attributed to inherent spatial soil variability, which is the variation of soil properties from one point to another in space due to different deposition and

Received 12 December 2002. Accepted 6 August 2001. Published on the NRC Research Press Web site at http://cgj.nrc.ca on xx xxxx 2003.

**T. Elkateb, R. Chalaturnyk,[1] and P.K. Robertson.** Department of Civil and Environmental Engineering, University of Alberta, Edmonton, AB T6G 2G7, Canada.

[1]Corresponding author (e-mail: rjchalaturnyk@civil.ualberta.ca).

 doi: 10.1139/T02-089 

loading history. Soil variability can have a profound effect on its behavior under earthquake loading, as discussed by Fenton and Vanmarcke (1991) and Popescu et al. (1998). Quantitative treatment of this variability with respect to liquefaction assessment is important for geotechnical design, as classical deterministic techniques cannot account for the scatter of field data and their spatial correlation. Well-documented case histories offer an opportunity to explore options of quantifying the influence of soil heterogeneity on liquefaction assessment. One such case history, the Wildlife Site, Imperial Valley, California, U.S.A., provides an excellent source for such studies as it was subjected to several earthquakes throughout the late twentieth century. In addition, the site was instrumented by the US Geological Survey (USGS) and subsequently recorded a unique set of ground responses during the 1987 Elmore Ranch and Superstition Hill earthquakes.

Several studies have been carried out to investigate the ground response at the Wildlife Site during the Superstition Hill earthquake, where various evidences of liquefaction were observed across the site. One of the early attempts to analyse the pore pressure response in the ground at the site was carried out by Dobry et al. (1989). A nonlinear one-dimensional finite element program was used in the analysis and reasonable agreement was found between predicted and measured pore pressures. A limitation of the analysis was the use of a one-dimensional model, which could not capture the interaction and stress transfer between different soil columns. Baziar et al. (1992) analysed the observed lateral spread behavior, implementing Newmark's sliding block method of analysis. It was assumed that failure would occur only in the top sandy silt and silt layers and that the sliding block could only move towards the free face. The high sensitivity of predicted displacements to presumed failure mechanisms illustrated the uncertainties associated with the proposed methodology. Moreover, the assumption of a vertical free face may have dramatically influenced the predicted behavior.

Gu et al. (1994) studied the ground response at the site with emphasis on the delayed development of pore pressure recorded by the piezometers after the strong motion had seized. That delayed response was attributed to stress redistribution within the ground and the onset of static liquefaction following the period of strong ground motion. The stress redistribution was analysed using the static finite element method implementing a simplified undrained boundary surface model and hyperbolic strain softening relationship. In addition, an elastic model was adopted to simulate the ground response during the reconsolidation stage. The main shortcoming of the analysis was the assumption that soil had been brought to the collapse surface everywhere across the site by the earthquake. Moreover, the authors believe that the delayed pore pressure development could be attributed to other factors, such as heterogeneous ground conditions leading to increased pore pressures within loose zones some distance from the piezometer locations.

Zeghal and Elgamal (1994) carried out a simplified analysis of the ground behavior using acceleration and pore-water pressure records during the 1987 Elmore Ranch and Superstition Hill earthquakes. Shear strain was assumed constant within the top 7.5 m of the ground, and linear interpolation was used to determine the shear stress at the location of the piezometer readings. The estimated shear stress and strain histories together with pore pressure measurements were used to investigate the mechanisms of nonlinear hysteretic soil response and pore pressure buildup. The major drawback of the analysis was the approximation associated with the assumption of constant shear strain across the ground. As well, the linear interpolation of shear stress does not agree with the fact that a different soil type exists in the top 2.5 m of the ground.

Recently, Beaty and Byrne (1998) re-investigated the ground response at the Wildlife Site using a simplified elasto-plastic constitutive model. The model was implemented into a one-dimensional finite difference analysis using the FLAC software (Itasca Consulting Group 1993), where the recorded downhole motion in the north–south direction was applied at the base of the model. The analysis showed reasonable agreement between the predicted and recorded seismic response prior to liquefaction, and the time of liquefaction onset was accurately forecasted. Predicted postliquefaction behavior, however, was found to be substantially different from field records.

To the authors' knowledge, the only attempt that was made to incorporate spatial variability of soil properties at the site in a probabilistic analysis framework was the pioneer study by Fenton and Vanmarcke (1991). Stochastic modeling of soil properties, such as permeability, porosity, modulus of elasticity, Poisson's ratio, and friction angle, was carried out using Monte Carlo simulation techniques. Different realizations of soil properties were implemented in one-dimensional finite element analyses with earthquake excitation applied at the base of the model. The effect of the limit of spatial correlation between soil properties on ground response was discussed together with the influence of connectivity of liquefied zones. In addition, a critical threshold of the area ratio of liquefiable zones was suggested to be associated with a high risk of liquefaction occurrence. A limitation of the study was the assumption of a homogeneous soil profile. As well, the influence of the spatial correlation structure model type on ground response was not accounted for.

In this study, a simplified geostatistical approach was adopted to assess the effect of lithological heterogeneity and spatial variability of soil properties on earthquake-induced ground response at the Wildlife Site. Cone penetration test (CPT) results applying the soil behavior type index, $I_c$, were used to identify different lithologies, for which statistical properties and spatial correlation characteristics were estimated. The cyclic stress ratio – cyclic resistance ratio (CSR–CRR) approach (Robertson and Wride 1998) was employed stochastically to estimate the liquefaction susceptibility of the ground. This was accomplished by implementing Monte Carlo simulation techniques to obtain several realizations of CPT data across the Wildlife Site. On the other hand, the earthquake loading was assessed deterministically using simplified techniques that correlated CSR to earthquake magnitude and maximum recorded surface acceleration. It should be noted that earthquake loading can be treated as a random variable, yet it was estimated in a deterministic fashion in this study as the Wildlife Site has experienced several earthquakes with known magnitude and surface accelerations. In addition, different procedures were used to assess the level of liquefaction damage, such as total damage potential and settlement criterion. A primary focus of these assessments was to ascertain whether methods could be developed for estimating representative soil parameters that can be used in simplified deterministic liquefaction analyses while continuing to honor the detailed ground heterogeneity.

## Background on the Wildlife Site

The Wildlife Site is located on the west side of the Alamo River, Imperial Valley, CA. Several earthquakes, with magnitudes ranging from 5 to 7, have shaken the site during the twentieth century, as shown in Table 1. The site showed signs of liquefaction during the 1950 and 1981 Westmoreland earthquakes, and as a result it was investigated and instrumented by the USGS to record ground response during future earthquakes, as shown in Fig. 1. The geology at the site was described by Bennett et al. (1984) based on the results of several laboratory and field tests. The top 12 metres consist of a surface layer of interbedded sandy silt, silt, and clayey silt to a depth of 2.50 m; followed by a loose sandy silt to silty sand up to a depth of 6.80 m; underlain by medium to stiff clayey silt to silty clay. The groundwater table was found to be at depth of 1.20 metres below ground surface. Site instrumentation, as described by O'Rourke and Hamada (1992), consisted of two accelerometers, one at the ground surface and the other at a depth of 7.50 m. In addition, six piezometers were installed to monitor pore pressure response together with an inclinometer and several survey points to capture expected lateral spread. The ground responses during the 1987 Superstition Hill and Elmore Ranch earthquakes were captured by the field instrumentation. These records showed an increase in pore-water pressure up to the value of the total geostatic pressure in response to the Superstition Hill earthquake. In addition, a maximum of 232 mm lateral spread of the ground, obtained from survey points, was measured together with the development of surface cracks and sand boils, as shown in Fig. 2.

## Characterization of ground heterogeneity

Characterization of ground heterogeneity at the Wildlife Site was carried out in three stages. In the first stage, standardization and filtration procedures were implemented to the CPT data. In the second stage, geostatistical characteristics of the standardized data were quantified. Finally, stochastic simulation of the standardized data was performed in the third stage. Details of these stages are discussed in the following sections.

### Standardizing cone penetration test data

The results from 11 cone penetration tests were used to characterize both the lithological and inherent property variability at the Wildlife Site. The CPT data were used to identify different ground lithologies using the soil behavior type index, $I_c$, (Robertson 1990), which was obtained through the relation

$$[1] \quad I_c = \sqrt{(3.47 - Q)^2 + (\log F + 1.22)^2}$$

where $Q$ and $F$ are the normalized CPT tip resistance and sleeve friction, respectively. They can be determined through $Q = (q_c - \sigma_v)/\sigma'_v$ and $F = f_s/(q_c - \sigma_v)$ where $q_c$ is the CPT tip resistance; $f_s$ is the CPT sleeve friction resistance; and $\sigma_v$ and $\sigma'_v$ are the total and effective vertical overburden pressure at the location of the CPT reading, respectively.

The soil behavior type index, $I_c$, can be used to classify soils according to their behavior type, as shown in Table 2. By applying this concept to different CPT data recorded at the Wildlife Site, a detailed east–west longitudinal ground profile was obtained, as shown in Fig. 3. Four cohesionless soil layers below the groundwater table (GWT), $L_1$, $L_2$, $L_3$, and $L_4$, were identified from the calculated values of $I_c$ and by implementing the soil classification system presented in Table 2. These layers, denoted by soil behavior types 5 and 6, were regarded as potentially liquefiable zones. Each of these layers was considered as a statistically homogeneous domain, where cone tip resistance, $q_c$, was treated as a random variable. It should be noted that zones associated with $I_c > 2.6$, denoted by soil behavior types 2–4 in Fig. 3, were assumed to be nonliquefiable layers (Robertson and Wride 1998).

Data filtration is an important process used to maintain statistical consistency within CPT data as it is possible that the soil being tested includes anomalies, such as very thin lenses of clay or sand, or pockets of gravel (Campanella et al. 1987). In this study, the filtration process was carried out by excluding such inhomogeneities, which were manifested in the form of spikes in CPT data at certain depths, following the procedure proposed by Harder and Van Bloh (1988). Each soil layer was divided into sublayers of 0.30 m thickness for which the mean $m$ and the variance $\sigma^2$ of cone tip resistance data were determined. Outliers were identified as values of $q_c$ that lie outside the range of $m \pm 2\sigma$. These values were excluded from the data set for each of the potentially liquefiable layers. In addition, upper and lower limits of $m \pm 2\sigma$ were proposed for the remaining data so that cone tip resistance cannot be greater than $m + \sigma$ or smaller than $m - \sigma$.

A necessary condition for the variogram modeling technique used in this study, as outlined in the next section, is stationarity, which implies that the geostatistical properties of random variables, such as mean and variance, do not depend on their location in space. It can be expected, however, that CPT data will exhibit vertical trends due to their sensitivity to changes in effective confining pressure. To use cone tip resistance, $q_c$, as a random variable and meet the stationarity condition, any possible vertical trend in $q_c$ should be removed (detrended). To achieve this, filtered data from all CPT soundings were utilized to identify deterministic linear vertical trends in $q_c$ within each of the four potentially liquefiable layers using regression analysis. These trends were then removed, as illustrated in Fig. 4, producing the detrended data for each of these layers through the relation

$$[2] \quad q = q_c - q_o(z)$$

where $q$ is the detrended cone tip resistance and $q_o(z)$ is a deterministic vertical trend.

It should be realized that the linear variation of vertical trends with depth shown in Fig. 4 is a simplifying assump-

**Table 1.** List of major earthquakes in the Imperial Valley in the twentieth century (modified from O'Rourke and Hamada 1992).

| Date | Richter magnitude | Recorded maximum surface acceleration | Occurrence of liquefaction |
|---|---|---|---|
| April 1906 | 6.00 | N/A | No |
| June 1915 | 6.30 | N/A | No |
| May 1917 | 5.50 | N/A | No |
| January 1927 | 5.80 | N/A | No |
| May 1940 | 6.40 | N/A | Yes |
| May 1940 | 5.50 | N/A | No |
| October 1979 | 6.60 | N/A | No |
| April 1981 (Westmoland earthquake) | 5.6 | N/A | Yes |
| November 1987 (Elmore Ranch earthquake) | 6.2 | 0.13$g$ | No |
| November 1987 (Superstition Hill earthquake) | 6.6 | 0.21$g$ | Yes |

**Note:** N/A indicates data not available.

**Fig. 1.** Layout of locations of CPT soundings and boreholes at the Wildlife Site (modified from Bennett et al. 1984).

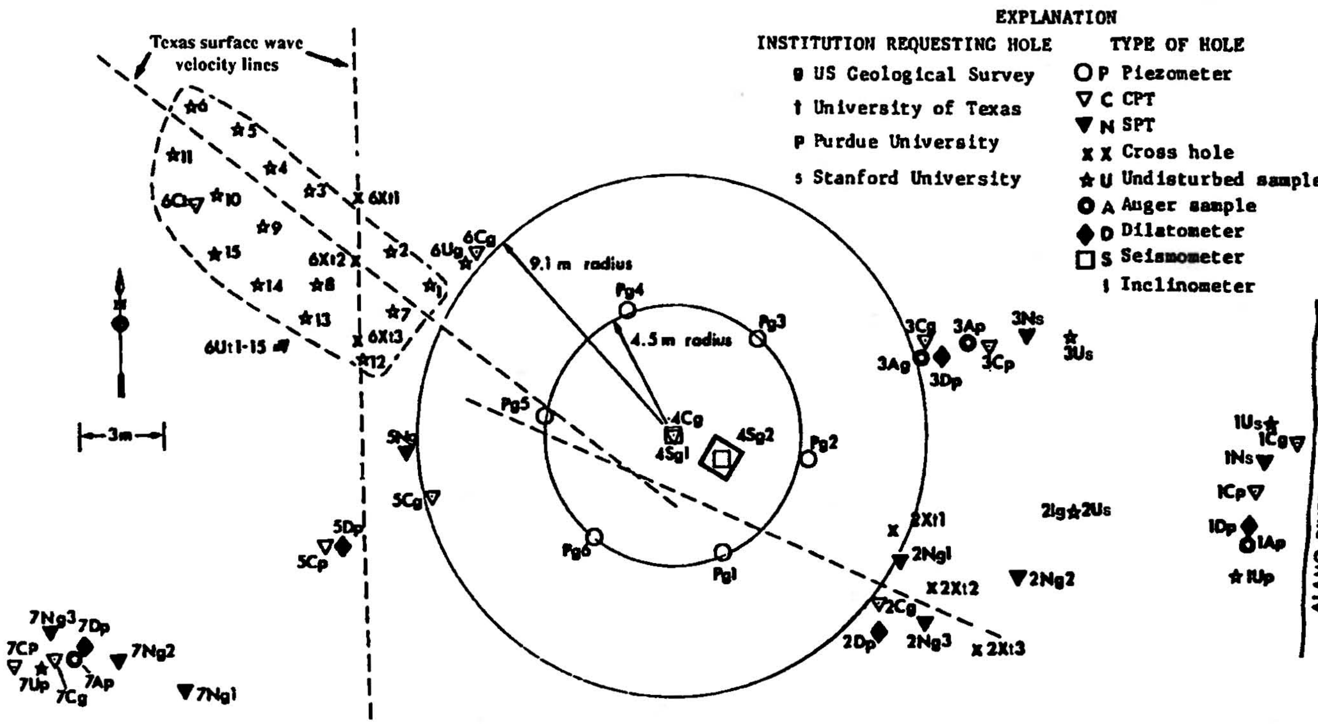


tion for practical application; as such variation can take other forms, especially for sandy soils. This assumption, however, has been used in several geostatistical studies in geotechnical engineering literature, such as Campanella et al. (1987) and Popescu et al. (1998). In addition, the uncertainty associated with the assessment of these vertical trends may have a significant influence on the site response under earthquake loading. However, this uncertainty decreases with increasing field data, as is the case for CPT data, and quantifying its effect is beyond the scope of this paper and needs to be considered in future studies.

## Geostatistical characteristics of detrended CPT data

To proceed with stochastic analyses, statistical characteristics of different random variables, such as mean, variance, probability distribution, and correlation structure, must be determined. A summary of the geostatistical characteristics of detrended CPT data for layers $L_1$ to $L_4$ is presented in Table 3. The mean values were found to be around zero, as expected, whereas the standard deviations ranged from 849 to 1570 kPa. The probability distributions were in close agreement with normal distributions as concluded from the Q–Q plots (Deutsch 2002) shown in Fig. 5. The Q–Q plots are comparisons between quantiles, which correspond to certain percentiles of the random variable, obtained from the probability distribution of field data and those of a reference distribution, such as the normal distribution as in this case study. If the cross plot between the two sets of quantiles results in points close to a 45° line, this indicates a similar shape and variance of both distributions.

Soil properties do not usually vary randomly in space; rather such variation is gradual and follows a pattern that

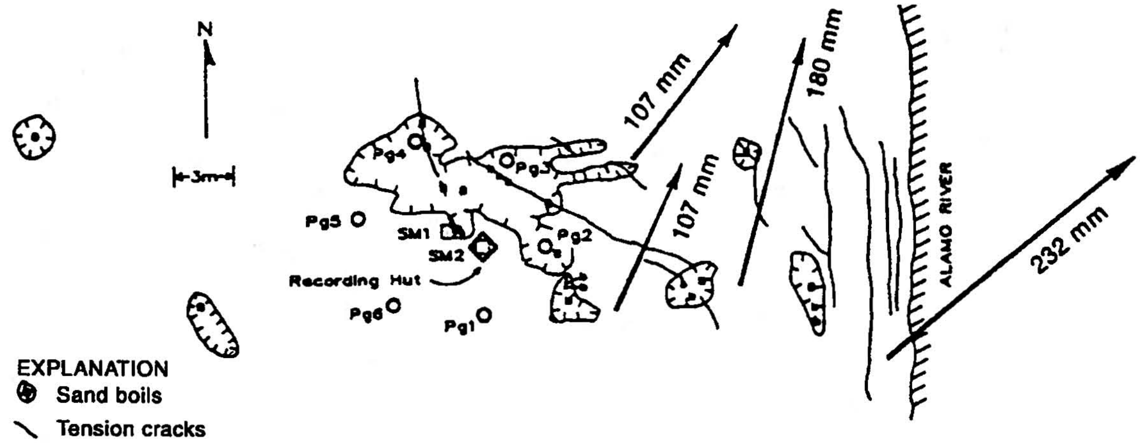


**Fig. 2.** Field records of lateral spreads, sand boils, and ground cracks at the Wildlife Site (modified from O'Rourke and Hamada 1992).

**Table 2.** Classification of soil using the soil behavior type index, $I_c$ (modified from Robertson and Wride 1998).

| $I_c$ | Soil behavior type | Description |
|---|---|---|
| <1.31 | 7 | Gravelly sand to dense sand |
| 1.31–2.05 | 6 | Clean sand to silty sand |
| 2.05–2.60 | 5 | Silty sand to sandy silt |
| 2.60–2.95 | 4 | Clayey silt to silty clay |
| 2.95–3.60 | 3 | Silty clay to clay |
| >3.60 | 2 | Organic soils |

can be quantified using what is called spatial correlation structure. This structure can be expressed in terms of the variogram or the covariance function. The variogram is a measure of dis-similarity between two points in space separated by a distance $h$, whereas the covariance is a measure of similarity between these points. In this study, variogram functions were adopted as measures of quantifying spatial correlation between detrended CPT data. They were determined through the relation

$$[3] \quad 2\gamma(h) = \mathrm{Var}[Z(u + h) - Z(u)]$$

where $2\gamma(h)$ is the variogram value at a separation distance $h$; $Z(u)$ is the value of the random variable, $q$, at location $u$; $Z(u + h)$ is the value of the random variable, $q$, at a distance $h$ from $Z(u)$; and Var[] is the variance operator.

Variograms are usually characterized by their model types and spatial ranges (Deutsch 2002). The variogram model is a parametric relationship used to curvefit the experimental variograms obtained from the analysis of field data. Examples of these variogram models, such as spherical, exponential, and Gaussian models, are shown in Fig. 6 in the companion paper (Elkateb et al. 2002). These models help determine the variogram at any separation distance and in different directions. In addition, they can incorporate other geological information, such as direction of maximum continuity, and maintain numerical stability of stochastic simulation (Deutsch 2002). Variogram range is a measure of the limit of spatial continuity of soil properties and can be defined as the separation distance at which the variogram reaches the sill (variance).

The GSLIB Geostatistical Software Library (Deutsch and Journel 1998) was used to obtain the variogram characteristics in both vertical and horizontal directions for each of the four layers, $L_1$ to $L_4$, as shown in Table 3. This was carried out by assessment of the normal score variogram values at several separation distances, as shown in Fig. 6, for detrended CPT data in the vertical direction. The normal score variogram is the variogram obtained from transforming detrended CPT data from their field distribution into a reference standard normal distribution of zero mean and unit variance (Deutsch and Journel 1998). Then, an iteration process was followed to obtain a theoretical variogram model that curvefit the variogram of transformed field data together with its spatial range, as shown in Fig. 6. Detailed descriptions of the different methods used to assess variogram spatial ranges is provided in the companion paper (Elkateb et al. 2002). It should be noted that variogram characteristics obtained from analysis of CPT data are, generally, sensitive to deposition conditions, loading history, and variation in fines content. This can explain the variation in variogram characteristics from one layer to another, as seen in Fig. 6.

One limiting boundary condition required to use GSLIB to obtain variogram characteristics is that each of the potentially liquefiable layers has to be rectangular in shape, as it is an extremely complicated process to obtain variogram characteristics using a nonorthogonal coordinates system. Consequently, a coordinate transformation process was carried out for each layer, as shown in Fig. 7, following the procedure of Deutsch (2002). Another objective of this transformation process was to retain spatial continuity between field data, as nontransformed sections may result in underestimated variogram ranges in the horizontal direction. This can be explained using Fig. 7, where variogram values cannot be assessed at a separation distance equal to AB*, as points A and B* exist in 2 different layers, which implies that the variogram range cannot be greater than the separation distance AC. On the other hand, variogram values can be assessed at any separation distance in the horizontal direction in the transformed section, as seen in Fig. 7. It should be realized, however, that this transformation process might result in some inherent uncertainty in variogram characteristics and consequently affects the results of stochastic

**Fig. 3.** An east–west view showing the lithological distribution across the Wildlife Site. (Position of cone wells are shown in Fig. 1; numbers between brackets represent soil behavior type based on the soil behavior type index, $I_c$; dimensions are in metres.)

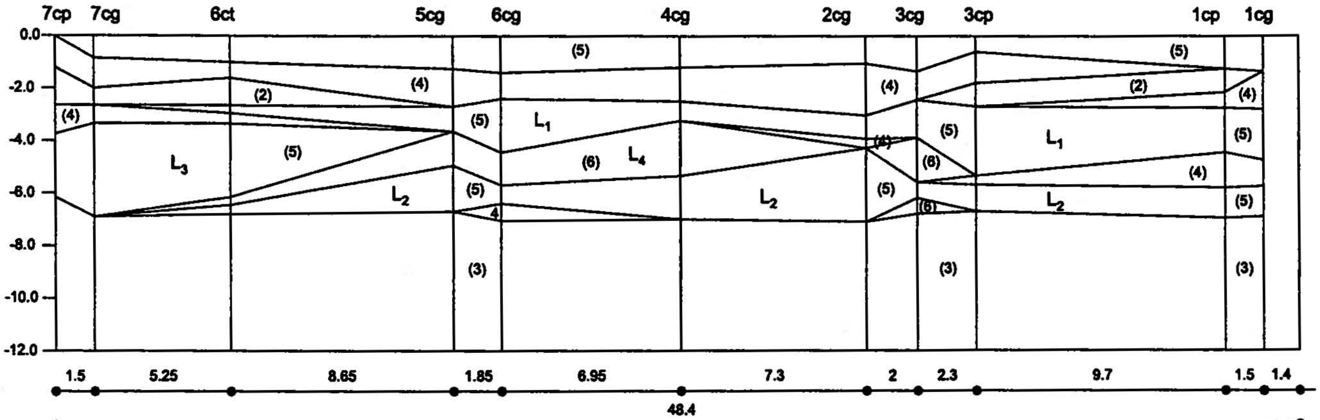


liquefaction analyses. Quantification of this uncertainty is beyond the scope of this simplified study.

For the Wildlife Site, insufficient data were available to reliably assess the horizontal anisotropy in variogram characteristics for different potentially liquefiable layers. As a result, it was assumed that the variograms would exhibit isotropic behavior in the horizontal direction, i.e., variogram characteristics did not depend on the azimuth in the horizontal direction. Furthermore, it was assumed that the horizontal variogram had the same model type as the vertical one, but with a larger range, as suggested by Deutsch (2002).

## Stochastic simulation of detrended CPT data

To quantify the effect of soil spatial variability on liquefaction susceptibility, several realizations of the detrended CPT data were obtained for each of the potentially liquefiable layers, $L_1$ through $L_4$. This was carried out implementing Monte Carlo simulation using the @Risk software (Palisade Corporation 1996), where each outcome of the simulation process was regarded as a representative (average) value of cone tip resistance for the layer under consideration. The number of realizations, about 10 000, was obtained through specifying an acceptable tolerance, around 0.50%, between the input distribution and the distribution of the sampled values of detrended CPT data obtained from the @Risk software.

It should be emphasized that the variance used in Monte Carlo simulation for each of the four potentially liquefiable layers was not the point (field) variance shown in Table 3. Rather, it was the variance of the spatial average of CPT data over selected averaging volumes. These spatial averages typically have a narrower probability distribution function than point statistics (Vanmarcke 1977) and consequently a smaller variance, as shown in Fig. 8. The variance of these spatial averages could be correlated to the point (field) variance using a variance reduction factor (Vanmarcke 1984) through the following relationship:

$$[4] \qquad \sigma_\Gamma = \Gamma_v^2 \sigma$$

where $\sigma$ is the standard deviation of field data (square root of point variance); $\sigma_\Gamma$ is the standard deviation of the spatial average of data over volume $v$; and $\Gamma_v^2$ is the variance reduction factor.

The variance reduction factor depends on the averaging volume, type of correlation structure, and the limit of spatial correlation between field data. Several analytical expressions for the variance reduction factor have been developed in geotechnical engineering literature. A summary of these expressions is provided in eqs. [7] and [9] in the companion paper (Elkateb et al. 2002). It should be noted that the lateral extent of a liquefied zone required to cause damage to overlying structures is usually small compared to the spatial range of horizontal variograms. For example, a sand boil of 1 m diameter may cause a significant damage to the overlying structure. Averaging CPT data over this small volume, compared with horizontal spatial range, which is typically in the range of tens of metres, will result in a variance reduction factor very close to 1 and consequently has a negligible influence on the outcome of Monte Carlo simulation. As a result, it was assumed in this study that the variance reduction factor would be affected only by the size of the averaging volume in the vertical direction, i.e., layer thickness. It is worth noting that the thicknesses of the four potentially liquefiable layers, $L_1$ to $L_4$ were not uniform across the site. As a result, an average thickness for each layer was obtained by dividing the volume contained between the upper and lower boundaries by the area covered by the layer. These average thicknesses were used to develop the variance reduction factors shown in Table 4.

The average thicknesses of layers $L_1$ and $L_4$ were divided into three and two horizontal sublayers, respectively, to avoid having high variance reduction factors that might affect the shape of the scaled probability distribution of CPT data of standard deviation equal to $\sigma_\Gamma$, as discussed by Deutsch (2002). It is worth noting that a minimum value of 0.70 for the variance reduction factor was recommended by Deutsch (2002) for use in stochastic analyses. Comparing this minimum value with the values used in the current study resulted in differences of about 5%, which was considered insignificant by the authors. However, the authors believe that there is a need to quantify the effect of selecting a specific averaging volume on the outcome of geostatistical liquefaction analysis in any future study. In addition, the average thick-

**Fig. 4.** Detrending of cone data; (*a*) identifying linear vertical trend and (*b*) detrended data.

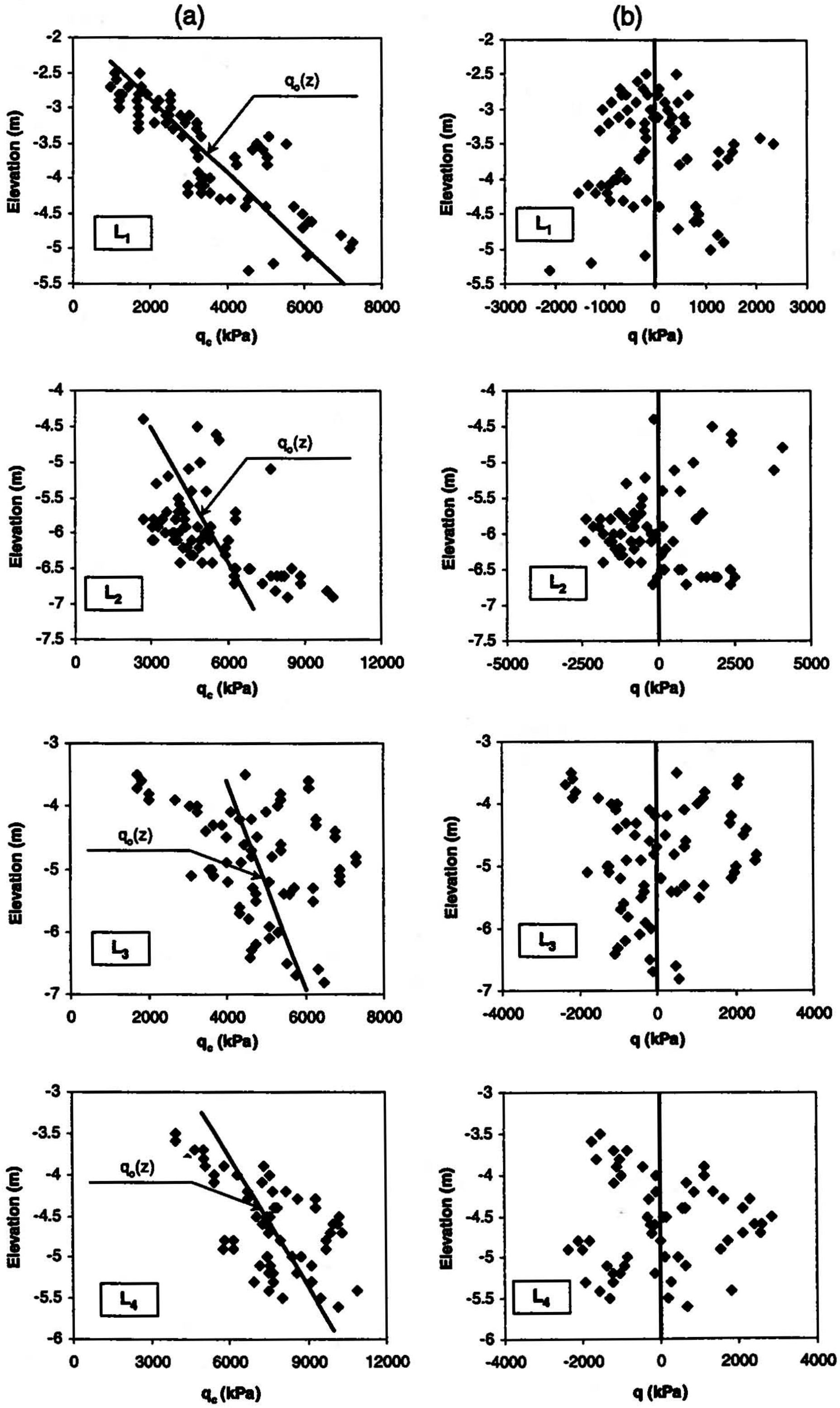


ness of layer $L_3$ was larger than the spatial range, $a$, of its spherical variogram, where the variance reduction factor developed by Elkateb et al. (2002) cannot be applied. As a result, this layer, as well, was divided into two sublayers. It should be emphasized that the outcomes of applying Monte Carlo simulation to different sublayers of any potentially liquefiable layer were not independent due to the vertical correlation between field data in these sublayers. The effect

**Table 3.** Statistical properties of detrended cone tip resistance data for different potentially liquefiable layers at the Wildlife Site.

| | | | Variogram characteristics | | | |
|---|---|---|---|---|---|---|
| Layer | Mean (kPa) | Standard deviation (kPa) | Model* | Nugget effect | Vertical range (m) | Horizontal range (m) |
| $L_1$ | –0.128 | 849.501 | Exponential | 0.05 | 0.55 | 10.00 |
| $L_2$ | –0.134 | 1567.03 | Spherical | 0.05 | 1.40 | 22.00 |
| $L_3$ | 0.036 | 1258.86 | Spherical | 0.05 | 1.45 | 22.00 |
| $L_4$ | 0.219 | 1333.85 | Exponential | 0.05 | 0.75 | 13.60 |

*For both horizontal and vertical directions.

**Fig. 5.** Q–Q plots comparing the actual probability distribution of field data and normal distribution for detrended cone tip resistance data.

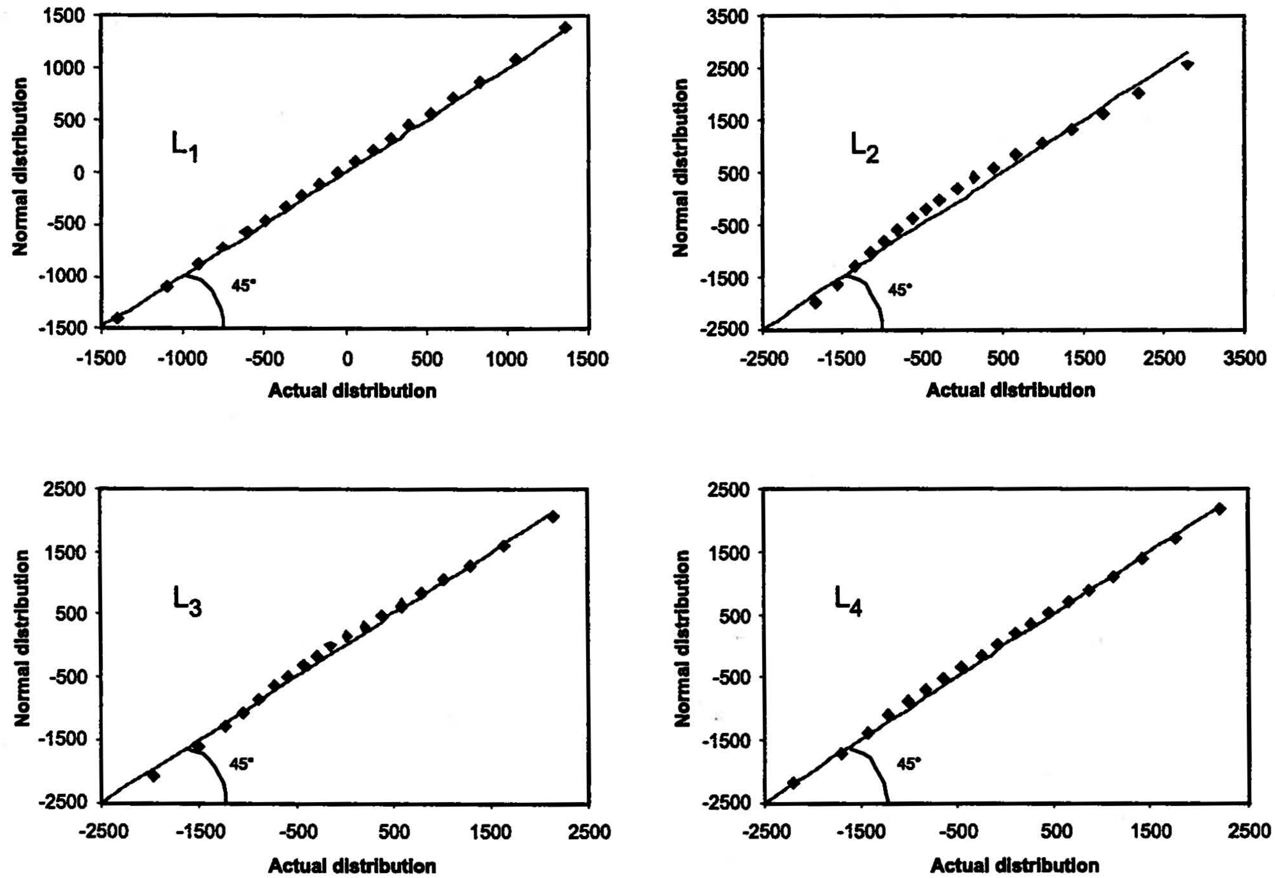


of such correlation was accounted for through implementing a correlation coefficient into the Monte Carlo simulation algorithm in the @Risk Software (Palisade Corporation 1996). As a result, the values of cone tip resistance sampled in every realization, for different sublayers, preserved the value of the correlation coefficient. This value was taken equal to the correlation coefficient between the spatial averages of CPT tip resistance data over a vertical distance equal to the thickness of each sublayer, as proposed by Vanmarcke (1984) and illustrated in eq. [10] in the companion paper (Elkateb et al. 2002).

## Stochastic analysis of liquefaction susceptibility

Stochastic analyses of liquefaction susceptibility of the ground at the Wildlife Site were performed by applying different realizations of retrended cone tip resistance data into a deterministic empirical approach. The retrended data were obtained by adding back the deterministic vertical trends to different realizations of the detrended CPT tip resistance data obtained from Monte Carlo simulations. The CPT-based empirical approach of Robertson and Wride (1998) was used in the analysis, where the factor of safety against liquefaction could be obtained through

$$\text{[5]} \quad F.S = \frac{CRR}{CSR}$$

where CRR and CSR are the cyclic resistance ratio and the cyclic stress ratio, respectively.

The cyclic stress ratio (CSR), the average normalized cyclic shear stress developed in the ground during the earthquake, was determined using the simplified approach of

Fig. 6. An assessment of vertical variogram characteristics for detrended CPT data using the GSLIB software.

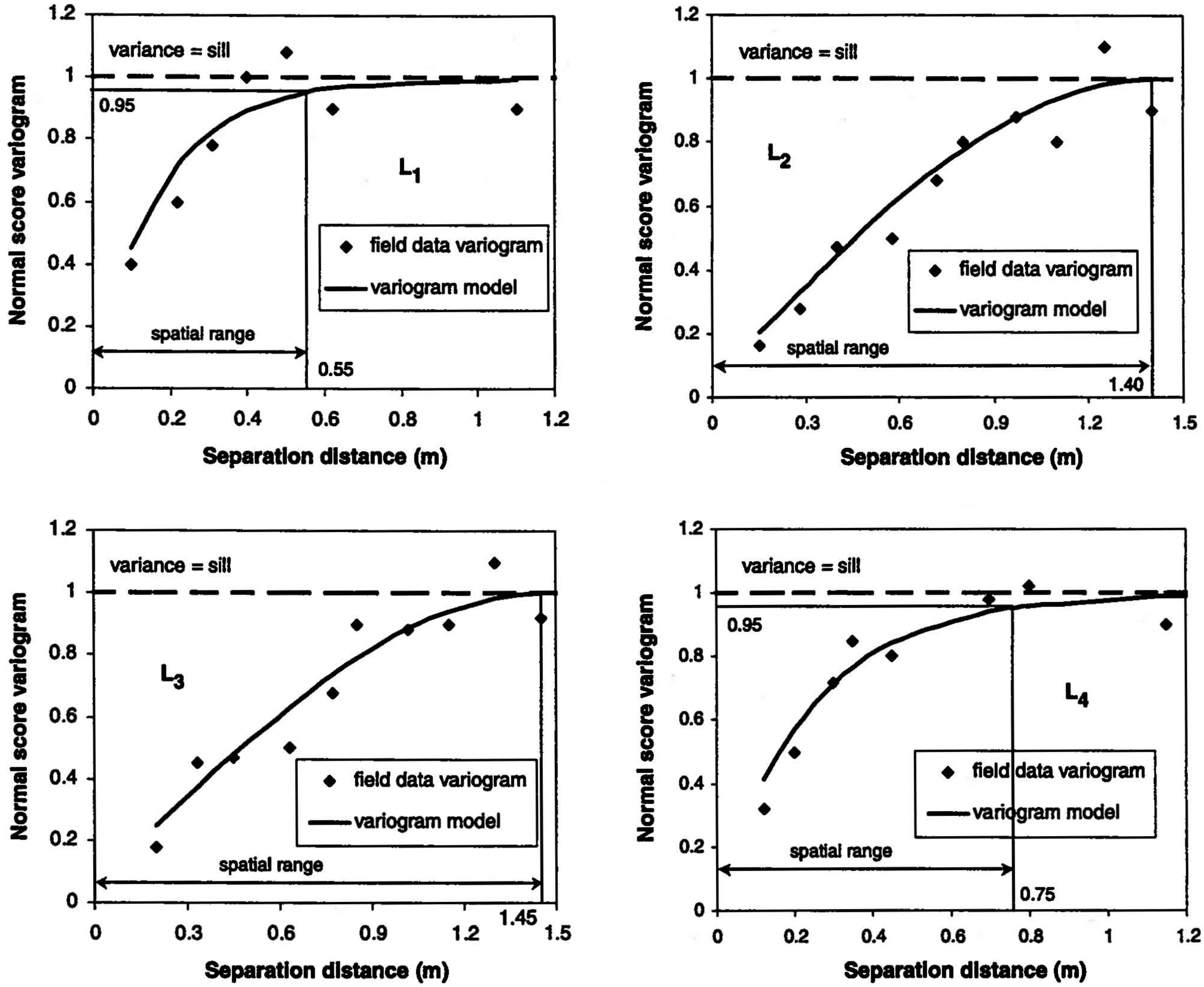


Fig. 7. Coordinate transformation process of potentially liquefiable layers.

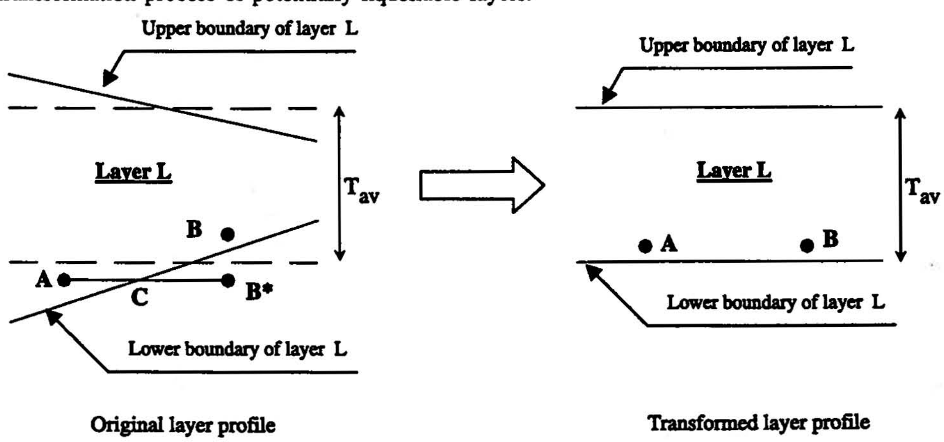


Seed and Idriss (1971) that relates CSR to earthquake magnitude and maximum surface acceleration through

$$[6]\quad \mathrm{CSR} = \frac{\tau_{av}}{\sigma'_v} = 0.65\left(\frac{a_{max}}{g}\right)\left(\frac{\sigma_v}{\sigma'_v}\right)r_d$$

where $a_{max}$ is the maximum acceleration at the ground surface; $g$ is the acceleration of gravity; $r_d$ is a stress reduction factor that depends on embedment depth; and $\sigma_v$ and $\sigma'_v$ are the total and effective vertical overburden pressures, respectively.

**Fig. 8.** The scaling of probability distribution of CPT data using the variance reduction factor and its effect on Monte Carlo simulation.

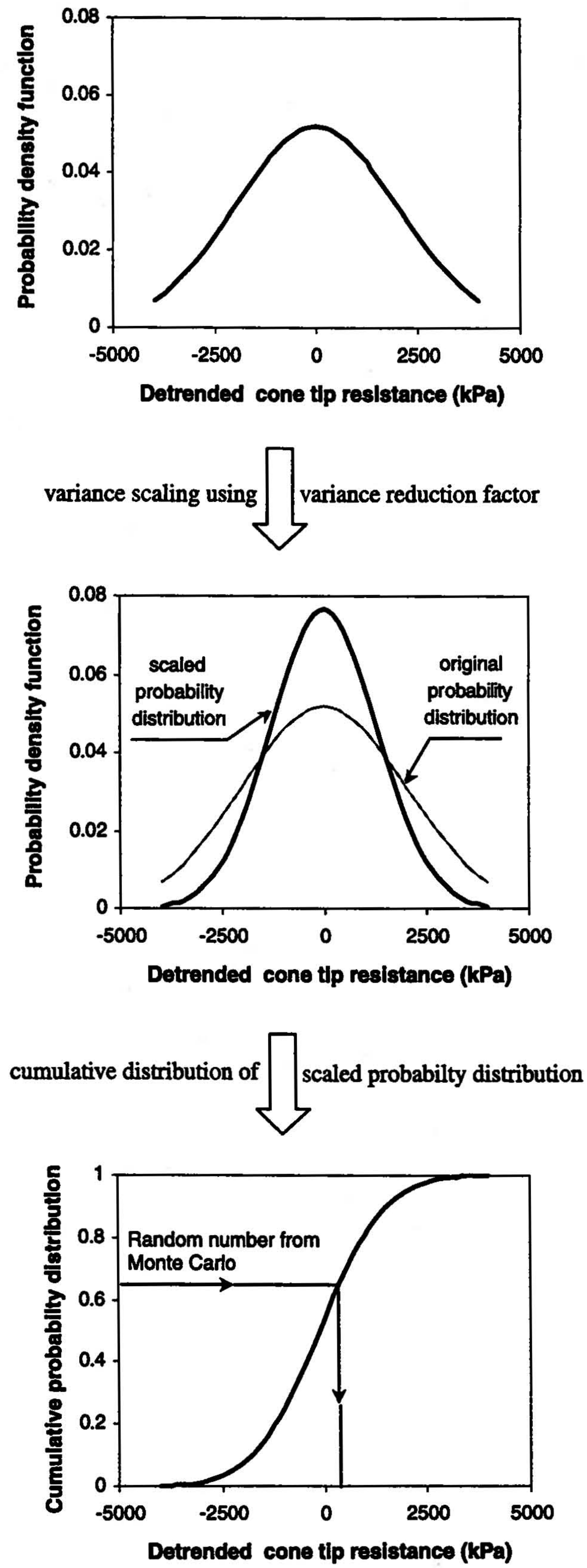


The cyclic resistance ratio (CRR) could be regarded as the average normalized shear stress required to cause cyclic liquefaction in the ground and was determined as proposed by Seed and Idriss (1971)

$$[7] \quad \mathrm{CRR} = \frac{\tau_{\mathrm{cr}}}{\sigma'_{\mathrm{v}}} = (\mathrm{CCR})_{7.5}\mathrm{MSF}$$

where $(\mathrm{CRR})_{7.5}$ is the cyclic resistance ratio for an earthquake of magnitude 7.5, and MSF is the magnitude scaling factor.

The cyclic resistance ratio of clean sand for an earthquake of magnitude 7.5 was determined using the empirical correlation proposed by Robertson and Wride (1998)

$$[8a] \quad (\mathrm{CRR})_{7.5} = 0.833\left(\frac{(q_{\mathrm{c1N}})_{\mathrm{cs}}}{1000}\right) + 0.05 \qquad (q_{\mathrm{c1N}})_{\mathrm{cs}} \le 50$$

$$[8b] \quad (\mathrm{CRR})_{7.5} = 93\left(\frac{(q_{\mathrm{c1N}})_{\mathrm{cs}}}{1000}\right)^3 + 0.08 \qquad 50 \le (q_{\mathrm{c1N}})_{\mathrm{cs}} \le 160$$

The term $(q_{\mathrm{c1N}})_{\mathrm{cs}}$ is the equivalent clean sand normalized cone tip resistance that accounts for the effect of grain characteristics, such as the presence of fines, which might result in higher liquefaction resistance due to the development of minor cohesion. This equivalent resistance can be assessed through

$$[9] \quad (q_{\mathrm{c1N}})_{\mathrm{cs}} = K_{\mathrm{c}}\, q_{\mathrm{c1N}}$$

where $K_{\mathrm{c}}$ is a correction factor that depends on grain characteristics; and $q_{\mathrm{c1N}}$ is the normalized cone tip resistance.

Both $K_{\mathrm{c}}$ and $q_{\mathrm{c1N}}$ were determined using the following relationships proposed by Robertson and Wride (1998):

$$[10] \quad K_{\mathrm{c}} = -0.403\, I_{\mathrm{c}}^4 + 5.581\, I_{\mathrm{c}}^3 - 21.63\, I_{\mathrm{c}}^2 + 33.75\, I_{\mathrm{c}} - 17.88$$

$$[11] \quad q_{\mathrm{c1N}} = \frac{q_{\mathrm{c}}}{\sigma'_{\mathrm{v}}}\sqrt{\frac{\sigma'_{\mathrm{v}}}{P_{\mathrm{a}}}}$$

where $I_{\mathrm{c}}$ is the soil behavior type index, as presented in eq. [1]; and $P_{\mathrm{a}}$ is the atmospheric pressure.

Several studies have been carried out to assess reasonable values for earthquake magnitude scaling factors (Seed and Idriss 1971; Ambrayses 1988; and Idriss 1995). Following the recommendation of NCEER 1996 (Youd et al. 2001), Idriss's modified scaling factor was adopted in this study in the form of

$$[12] \quad \mathrm{MSF} = \frac{10^{2.24}}{M^{2.56}}$$

where $M$ is the Richter magnitude of the earthquake.

The above relations were used to assess the ground response during the 1987 Superstition Hill earthquake ($M$ = 6.6) where the maximum surface acceleration recorded was approximately $0.21g$. Stochastic assessment of the factor of safety against liquefaction was carried out for each of the four layers using 10 000 realizations of retrended CPT data. The results of these analyses, as shown in Fig. 9, indicated

**Table 4.** Variance reduction factor for different potentially liquefiable layers at the Wildlife Site.

| Layer | $L_1$ | $L_2$ | $L_3$ | $L_4$ |
|---|---|---|---|---|
| Averaging thickness (m) | 1.17 | 1.19 | 2.04 | 1.02 |
| Variance reduction factor | 0.551 | 0.605 | 0.666 | 0.667 |

that the mean factors of safety for layers $L_1$ to $L_4$ were 0.75, 1.18, 1.12, and 1.56, respectively. The coefficients of variation were assessed to be 0.14, 0.29, 0.26, and 0.20. Whereas, the probabilities of failure (factor of safety less than unity), $P_F$, were found to be 98.8, 32.9, 37.5, and 3.2%, respectively.

Similar analyses were conducted for other earthquakes that had occurred at the site, such as the 1987 Elmore Ranch ($M$ = 6.2, $a_{max}$ = 0.13$g$), the 1981 Westmorland ($M$ = 5.6, $a_{max}$ = 0.22$g$), and the 1979 earthquake ($M$ = 6.6, $a_{max}$ = 0.115$g$). It should be noted that the maximum surface accelerations for both the 1981 and 1979 earthquakes were not recorded at the site. These surface accelerations were estimated through empirical relations that correlated maximum ground acceleration to earthquake magnitude and epicentral distances (Krinitzsky et al. 1988). A summary of the analysis results for these earthquakes is shown in Table 5.

Liquefaction occurred during the 1981 Westmoreland earthquake, in spite of the fact that the mean factors of safety for all layers at the site were larger than one. This implies that the use of mean values in a liquefaction analysis could be on the unsafe (nonconservative) side as a result of ignoring scatter in field data and spatial correlation between soil properties. Consequently, more meaningful representative values have to be identified to assess liquefaction susceptibility. Moreover, it is worth noting that liquefaction occurred at a failure probability of 37.7% for the shallowest layer compared to significantly smaller values, less than 8%, for deeper layers. This emphasizes the importance of embedment depth of liquefiable layers on liquefaction occurrence and suggests that depending on the factor of safety solely may not be an accurate measure of liquefaction potential. Conversely, liquefaction did not occur during the 1979 earthquake where the probability of failure of the shallowest layer was 2.5%. This implied that a critical probability of failure, ranging between 2.5 and 37.7%, could be identified for shallow layers above which liquefaction is likely to occur in sites of similar subsurface conditions. Studying additional case histories can help narrow the wide range of this critical threshold.

To account for the thickness and embedment depth of potentially liquefiable layers and their implications on liquefaction susceptibility, an estimate of equivalent (representative) probability of failure was developed in this study in the form of

$$[13] \quad P = \sum_{i=1}^{n} P_{Fi} \frac{T_i/Z_i}{\sum T_i/Z_i}$$

where $P$ is the equivalent failure probability of the site; $P_{Fi}$ is the probability of failure of layer $i$; $T_i$ is the average thickness of layer $i$; and $Z_i$ is the vertical distance from the ground surface to the center of layer $i$.

The above equation was used to estimate the equivalent failure probability under the effect of the Superstition Hill, Elmore Ranch, Westmoreland, and 1979 earthquakes, and was found to be 49, 1.2, 15.36, and 1.17%, respectively. This implied that an equivalent failure probability range of 1.2 to 15% could be identified as a critical threshold above which liquefaction would likely occur. This relatively wide range can be verified and refined through the analysis of more case histories.

It is worth noting that the empirical formulae used in this section involve some degree of inherent uncertainty. This is more significant in the CRR formula, where various degrees of engineering judgment were implemented in the assessment of different points used to develop the CRR formula (eq. [8]). Quantifying such uncertainty was considered to be a very complicated process beyond the scope of the current simplified study.

## Damage criteria of liquefaction

A major concern in liquefaction analysis is the impact of liquefaction occurrence in subsurface layers on overlying structures. Due to the complexity of the problem, few attempts have been made to quantify liquefaction-induced surface damage.

Iwasaki et al. (1978) proposed a damage criterion, based on several liquefaction case histories in Japan, where surface damage was assumed to be inversely proportional to the subsurface depth of liquefiable layers. A total liquefaction damage potential, $P_L$, was introduced through

$$[14] \quad P_L = \int_0^{20} D(z)\mathrm{d}z \qquad 0 \le P_L \le 20$$

where $D(z) = (1 - \mathrm{F.S})(10 - 0.5z)$ for $D(z) \ge 0$; F.S is the factor of safety against liquefaction; and $Z$ is the embedment depth in metres.

A value of $P_L$ less than 5 was found to be associated with minimal liquefaction damage to surface structures.

Another damage criterion was suggested by Ishihara and Yoshimine (1992) where liquefaction-induced damage was correlated to surface settlement. In their study, it was suggested that significant surface damage was usually associated with a ground settlement of 10 cm or more. Dobry (1994) proposed a relatively similar measure of liquefaction damage based on different types of ground displacements required to cause repairable or irreparable damage in overlying foundation upon earthquake loading, as listed in Table 6. This work was in agreement with that of Ishihara and Yoshimine (1992) in selecting 10 cm ground settlement as a lower limit for significant surface damage.

For the 1987 Superstition Hill earthquake, Iwasaki's damage criterion was applied to the 10 000 realizations of retrended CPT data, used in the previous section, and the total damage potential index, $P_L$, was determined at each CPT location. The results were used to generate contours of the probability that $P_L$ will be larger than 5 ($P_L > 5$), a threshold of $P_L$ associated with significant surface damage, as shown in Fig. 10. For the present study, it was assumed that sand boils and ground cracks identified zones of surface damage. The locations of these manifestation of liquefaction damage are shown in Fig. 10, where sand boils are represented by hatched zones, indicating that surface damage is likely to oc-

**Fig. 9.** Factors of safety against liquefaction for different potentially liquefiable layers at the Wildlife Site during the 1987 Superstition Hill earthquake. *m*, mean; COV, coefficient of variation, $P_F$, probability of failure.

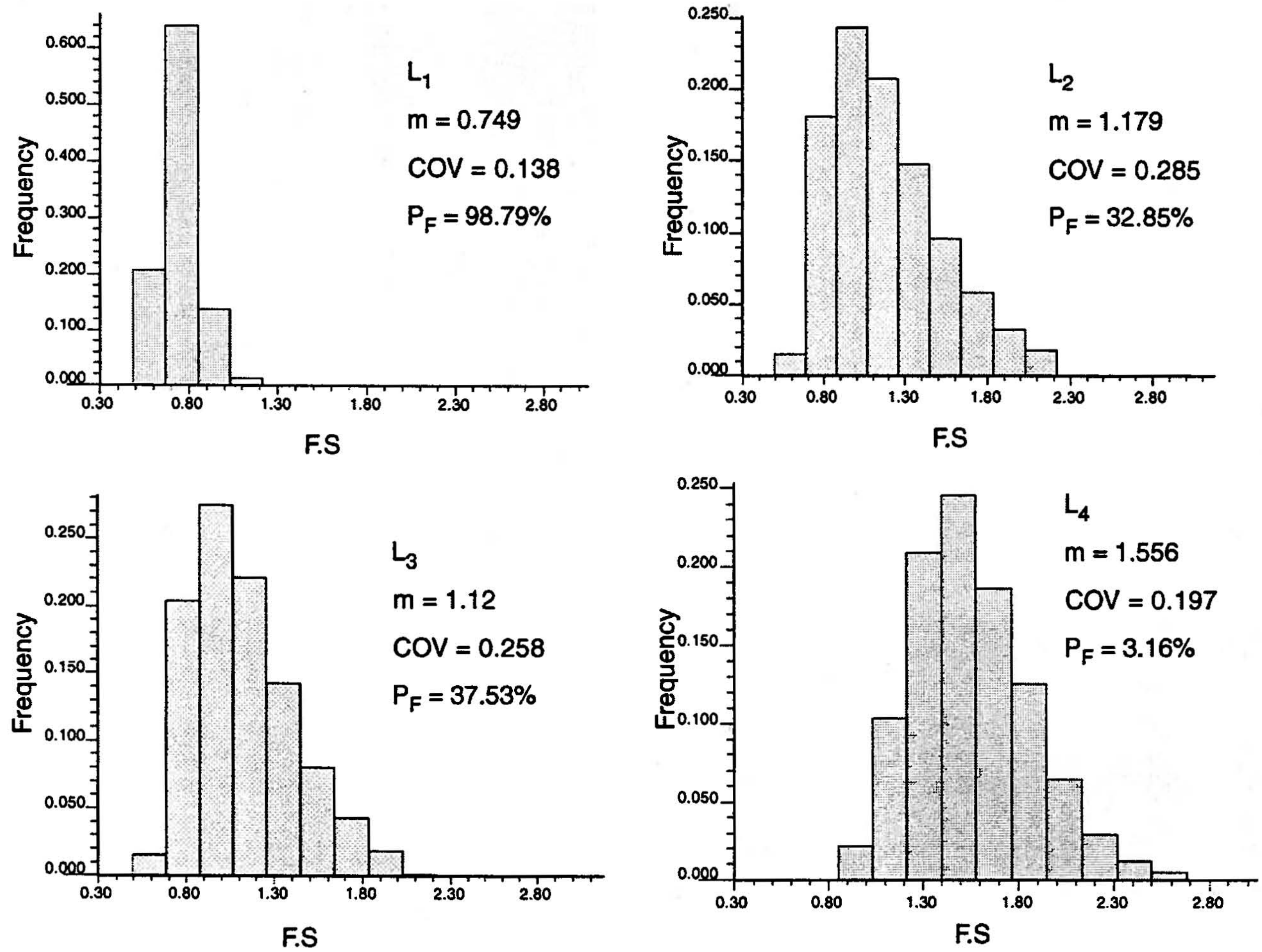


**Table 5.** Statistical characteristics of factors of safety against liquefaction for different earthquakes at the Wildlife Site.

| | | Layer | | | |
|---|---|---|---|---|---|
| Earthquake | F.S | $L_1$ | $L_2$ | $L_3$ | $L_4$ |
| Superstition Hill (1987) | Mean | 0.749 | 1.179 | 1.12 | 1.556 |
| | COV | 0.138 | 0.285 | 0.258 | 0.197 |
| | $P_F$ (%) | 98.79 | 32.85 | 37.53 | 3.16 |
| Elmore Ranch (1987) | Mean | 1.419 | 2.214 | 2.116 | 2.95 |
| | COV | 0.138 | 0.285 | 0.258 | 0.197 |
| | $P_F$ (%) | 1.35 | 1.89 | 1.36 | <0.01 |
| Westmoreland (1981) | Mean | 1.042 | 1.64 | 1.56 | 2.165 |
| | COV | 0.138 | 0.285 | 0.258 | 0.197 |
| | $P_F$ (%) | 37.65 | 7.82 | 7.46 | 0.34 |
| 1979 Earthquake | Mean | 1.365 | 2.346 | 2.182 | 2.836 |
| | COV | 0.138 | 0.285 | 0.258 | 0.197 |
| | $P_F$ (%) | 2.54 | 0.57 | 0.88 | <0.01 |

**Note:** $P_F$ is the probability of failure.

cur only if the probability of ($P_L > 5$) is larger than a critical threshold of about 1.2%.

To apply the damage criterion of Ishihara and Yoshimine (1992), ground settlements at the site under the effect of the Superstition Hill earthquake were estimated using the empirical approach proposed by Ishihara (1993). In this approach, earthquake-induced volumetric strain is correlated to the factor of safety against liquefaction and relative density, as

**Table 6.** Approximate ground displacements (in cm) required to cause repairable and irreparable damage (modified from Dobry 1994).

| | | Displacement required to cause | |
|---|---|---|---|
| Type of deformation | Foundation type | Repairable damage | Irreparable damage |
| Shear | Poorly reinforced | 0.10 | >0.30 |
| | Well reinforced | >0.30 | — |
| Extension | Poorly reinforced | <0.05 | >0.30 |
| | Well reinforced | >0.10 | — |
| Compression | Poorly reinforced | <0.30 | >0.50 |
| | Well reinforced | >0.50 | — |
| Compression with vertical | Poorly reinforced | <0.20 | >0.20 |
| | Well reinforced | <0.30 | >0.30 |
| Vertical | Poorly reinforced | <0.05 | >0.20 |
| | Well reinforced | <0.10 | >0.30 |

**Note:** — indicates data not available.

**Fig. 10.** A site plan showing contours of probability of occurrence of total liquefaction damage potential ($P_L$) greater than 5 for the Superstition Hill earthquake (hatched zones indicate observed sand boils at the site). Dimensions are in metres.

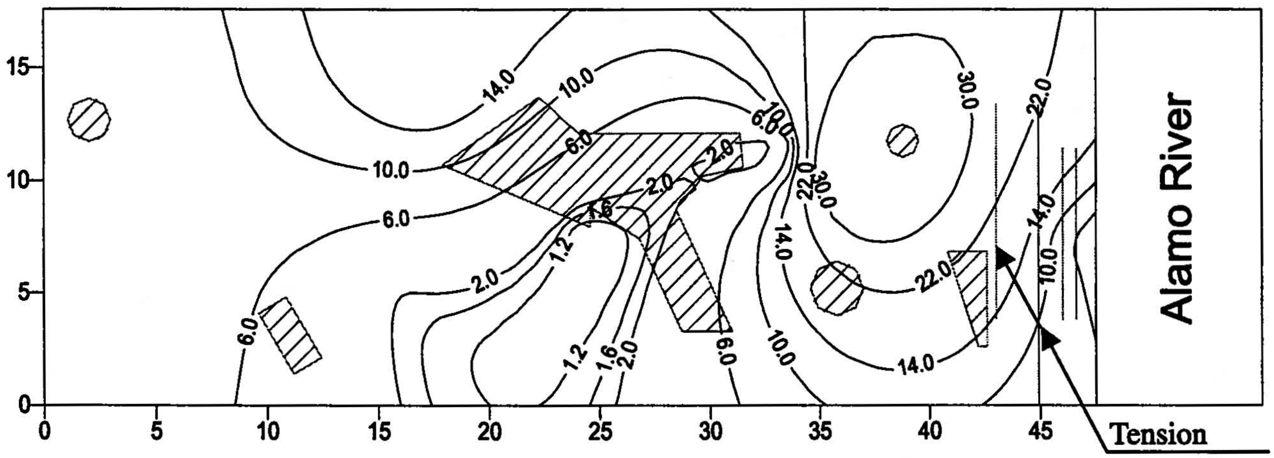


shown in Fig. 11. The relative densities of different soil layers were expressed in terms of normalized cone tip resistance, $q_{c1}$, where

$$[15] \quad q_{c1} = \frac{q_c}{\sqrt{\sigma'_v / P_a}}$$

The above 10 000 realizations of retrended CPT data were implemented into Ishihara's approach, and the associated settlements were determined resulting in a settlement histogram at each location of the CPT soundings. It was found that the value of mean settlements across the site ranged from 4.4 to 13.3 cm, whereas the coefficients of variation ranged from 0.18 to 0.86. A summary of the main characteristics of ground settlement histograms is provided in Appendix A. The settlement analysis results were used to compute the probability of occurrence of liquefaction-induced settlement greater than 10 cm, a value considered by Ishihara and Yoshimine (1992) to be associated with significant surface damage. Contours of the probability of settlements greater than 10 cm ($P_{10}$) were generated across the Wildlife Site, as illustrated in Fig. 12. It can be concluded from this figure that zones of surface damage are likely to be bounded by a 12% probability of occurrence of settlement larger than 10 cm.

Contours of computed mean settlements and those associated with the upper and lower limits of the 90% level of confidence for the Superstition Hill earthquake (1987) are shown in Fig. 13. A detailed discussion of the use of the 90% confidence level in stochastic geotechnical analyses is provided in the companion paper (Elkateb et al. 2002). This confidence level provides useful design guidelines as it implies that there is only a 10% chance of having ground settlements outside the range predicted using its upper and lower limits. In other words, there is a 5% chance of having settlements either larger than the upper limit or smaller than the lower limit. As expected, the use of mean values could be on the nonconservative side, as shown in Fig. 13, where the settlements associated with the upper limit of the 90% confidence level may be as high as 2.5 times the mean settlements. This can be attributed to the presence of loose pockets resulting in low factors of safety and higher settlements, which cannot be accounted for using classical deterministic analyses.

The above settlement analysis was repeated for other earthquakes that occurred at the Wildlife Site. Detailed results of these analyses are presented in Appendix A. For both the 1979 and the Elmore Ranch earthquakes, where no sign of liquefaction was recorded at the site, the analyses showed

**Fig. 11.** Postliquefaction volumetric strain as a function of factor of safety (modified from Ishihara 1993). $D_r$, XXXXXX; $N_?$, XXXXXX; $\gamma_{max}$, XXXXXX.

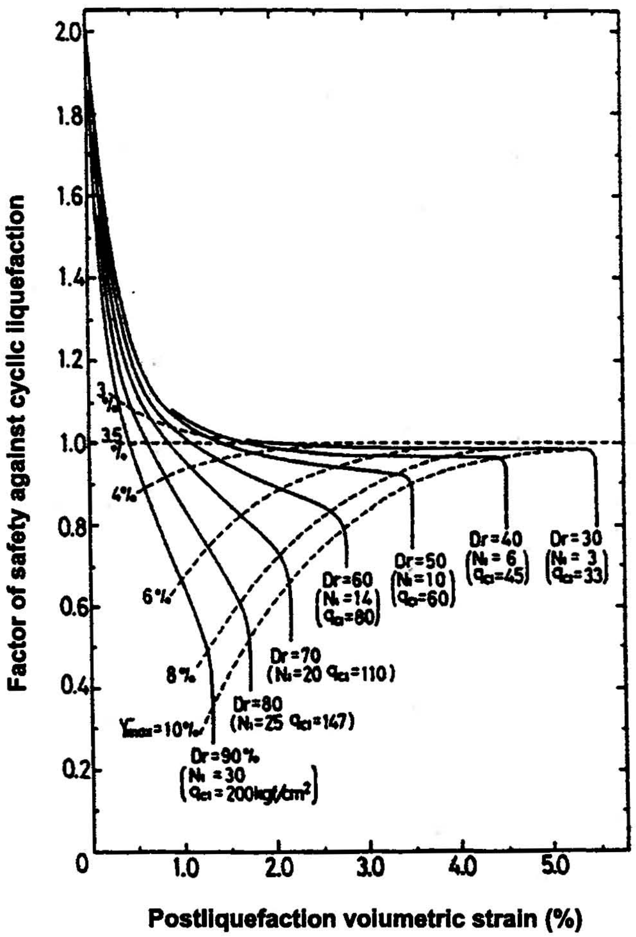


that there was insignificant probability, less than 0.01%, of occurrence of surface settlements larger than 10 cm. This implies that liquefaction is likely to occur if there is a chance of having a vertical settlement larger than 10 cm somewhere across the site. It should be realized, however, that these results were obtained using Ishihara's method for the assessment of liquefaction-induced settlement and should not be generalized for other cases where different methods are used for the assessment of ground settlement.

It is worth noting that the effect of nonuniformity in the thickness of different potentially liquefiable layers on the stochastic settlement analysis at each CPT sounding location was taken into consideration through rescaling of the outcome of Monte Carlo simulation. The rescaling process was carried out by transforming the outcome of Monte Carlo simulation from its original distribution to a reference distribution with the same type and mean value but with a modified variance, $\sigma_{mod}$. This variance depends on layer thickness at each CPT location according to

$$[16] \quad \sigma_{mod} = (\sigma)_{\Gamma}\, C_R$$

where $\sigma_{mod}$ is the modified variance at each CPT location, and $C_R$ is a correction factor.

The correction factor, $C_R$, was determined through

$$[17] \quad C_R = \frac{\Gamma_{vi}^2}{\Gamma_v}$$

where $\Gamma_{vi}^2$ is the variance reduction factor at each CPT location, as shown in Fig. 14.

## Representative parameters for deterministic analyses

The above methodology, while being amenable to engineering design, could be regarded as a relatively sophisticated process for engineers with limited statistical background. Moreover, relying on mean values may provide a nonconservative estimate of liquefaction potential, as discussed in the previous sections. To overcome these issues, an attempt was made to ascertain whether more representative soil parameters could be determined that honor detailed ground heterogeneity and could be used more reliably in simplified deterministic analyses.

As discussed in the previous section, liquefaction is unlikely to occur if there is insignificant (less than 0.01%) probability of having settlement of 10 cm everywhere across the site, as was the case for the Elmore Ranch and the 1979 earthquakes. As a result, it was suggested that a characteristic percentile of cone tip resistance that could be used for liquefaction prediction would likely be correlated with a settlement of 10 cm. In other words, such a characteristic percentile would not predict settlements greater than 10 cm anywhere across potentially liquefiable sites when used in simplified deterministic analysis under the effect of earthquakes that do not trigger liquefaction. Using this percentile was considered to provide a more rational basis for the assessment of liquefaction potential.

To obtain this deterministic percentile, contours of probability of occurrence of liquefaction settlement greater than 10 cm, $P_{10}$, under the effect of the 1981 Westmoreland earthquake were generated, as shown in Fig. 15. It was found that the surface area covered by $P_{10} > 0$ represented 89% of the effective statistical area of the site. The effective statistical area, $A_1$, can be defined as the rectangular surface area determined by the minimum and maximum horizontal coordinates of all CPT soundings taking the CPT sounding 7cp as the origin of coordinates, as shown in Fig. 16. In other words, this area extends from the CPT sounding 7cp as far north as the sounding 6ct and as far east as the sounding 1cg. Then, a series of deterministic settlement analyses was carried out using different percentiles of CPT tip resistance data. The characteristic percentile was assessed as that which would reproduce an area ratio of 0.89 for 10 cm settlement, i.e., the area covered by a ground settlement greater than 10 cm represented 0.89 of the effective statistical area, $A_1$. This procedure is shown in Fig. 17 where the characteristic percentile was found to be 0.085; i.e., 8.5% of CPT tip resistance data were found to be smaller than the characteristic $q_c$. It should be noted that the above procedure was not applied to other earthquakes recorded at the Wildlife Site, as these earthquakes resulted in $P_{10}$ being either negligible or more than zero everywhere across the site.

In a similar fashion, attempts were made to obtain a representative cone tip resistance value that could be used in a deterministic analysis to predict liquefaction-induced ground

**Fig. 12.** A site plan showing contours of probability of liquefaction-induced settlements greater than 10 cm for the Superstition Hill earthquake (hatched zones indicate observed sand boils at the site).

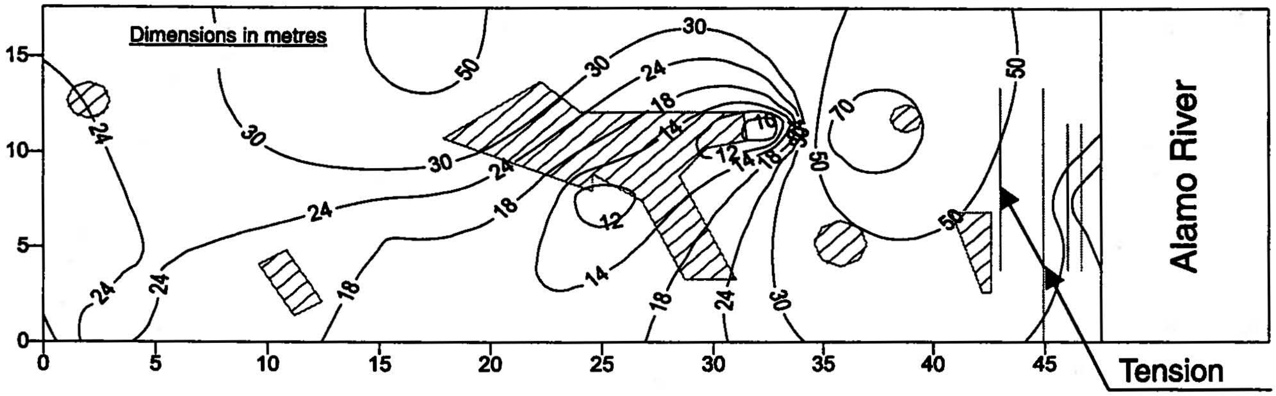


**Fig. 13.** A site plan showing contours of computed settlements (in cm) across the Wildlife Site under the effect of the Superstition Hill earthquake (*a*) mean settlement; (*b*) lower limit of 90% confidence interval; and (*c*) upper limit of 90% confidence interval.

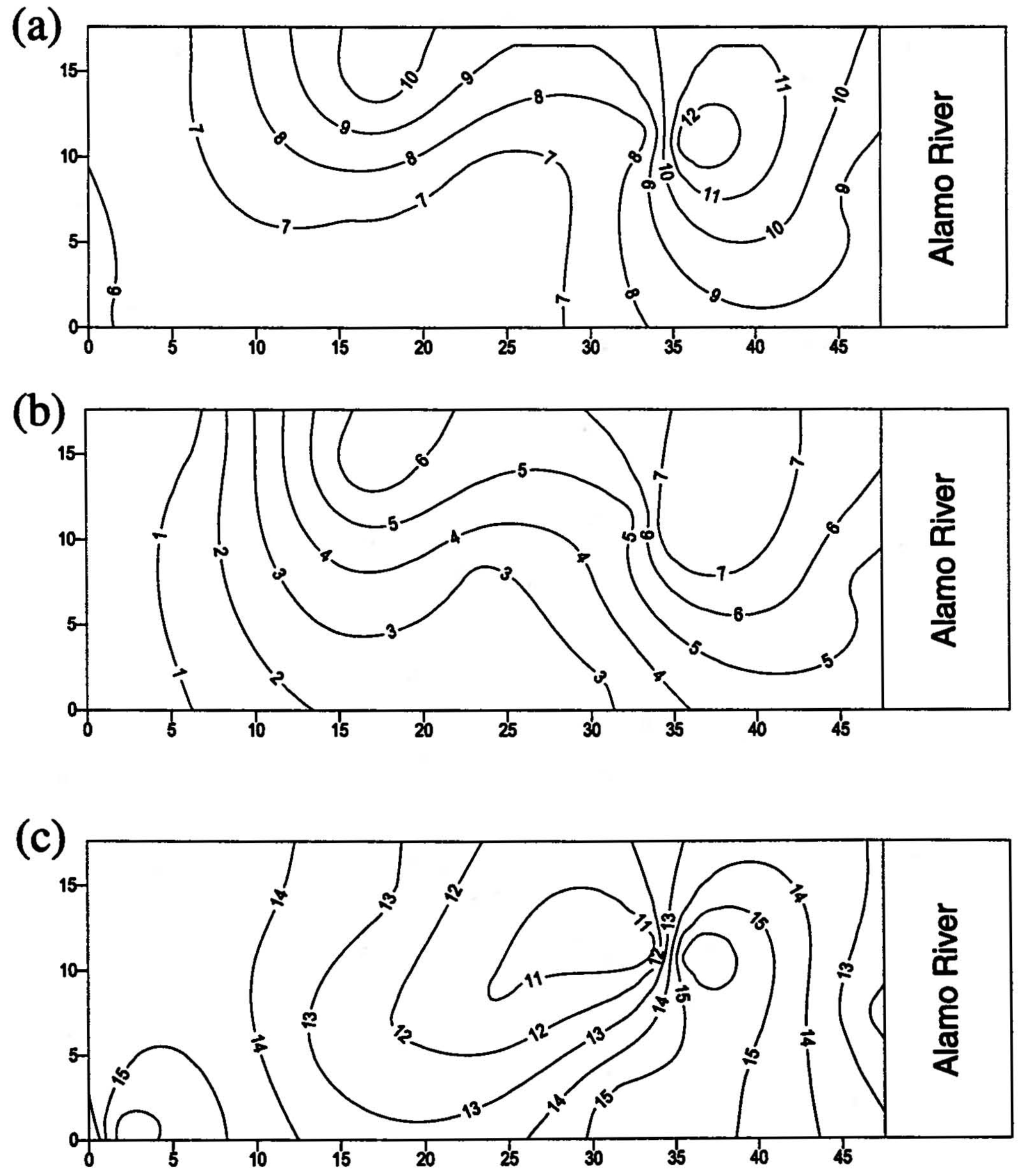

**Fig. 14.** Modified variance reduction factor at each CPT location.

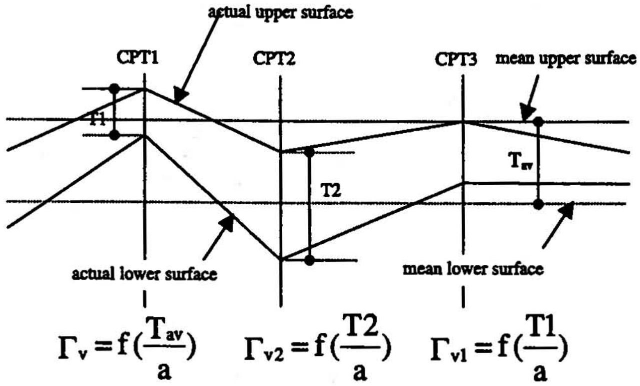


settlement associated with the upper limit of the 90% confidence level. In other words, upon using this representative value in a simplified deterministic analysis, liquefaction-induced settlement can be predicted with only a 5% chance that actual settlements would exceed the predicted values. To obtain this percentile, the volume change associated with the upper limit of the 90% confidence interval of ground settlement, $\Delta V_{90}$, was determined across the statistical effective area, $A_1$, and was found to be 105 m$^3$ for the 1987 Superstition Hill earthquake. Then, a series of deterministic settlement analyses was carried out using different percentiles of CPT data. The characteristic percentile was assessed as the percentile that would reproduce $\Delta V_{90}$, i.e., a volumetric change equal to 105 m$^3$. This procedure is shown in Fig. 18 where the characteristic percentile was found to be 0.29. Similar analyses were applied to the 1987 Elmore Ranch, 1981 Westmoreland, and the 1979 earthquake, where the characteristic percentiles were found to be 0.18, 0.20, and 0.17, respectively. This implied that no unique percentile of cone tip resistance could reproduce $\Delta V_{90}$ for the different earthquakes considered in this study. Rather, these percentiles were found to be dependent on the shear stresses generated in the ground upon earthquake loading and on whether or not the site would liquefy under the effect of these stresses. From the results obtained, however, it could be postulated that these percentiles range between 0.20 and 0.29 when liquefaction would be expected to occur, and range between 0.17 and 0.18 otherwise. The use of these percentiles can account for the presence of looser pockets in the ground, which are likely to have a great influence on the liquefaction potential of the site.

## Assessment of the degree of variability of potentially liquefiable sites

The results obtained from the previous section are valid for sites with similar subsurface conditions and geostatistical characteristics although they can be used as relatively conservative measures for sites of smaller variability. As a result, an empirical estimate was developed in this study as a qualitative measure to compare the degree of variability of potentially liquefiable sites. This estimate was expressed in terms of the overall variability factor, OVF, which is the weighted mean of the local variability factor, LVF, calculated at each CPT location. The weights used in the calculation of OVF were assessed based on the area of influence (tributary area) of each CPT sounding, as shown in Fig. 19. The LVF was estimated through

$$[18]\quad \mathrm{LVF} = \sum_{i=1}^{n} \frac{(\mathrm{COV})_i (D_\mathrm{F})_i (T_\mathrm{N})_i}{(R_\Gamma)_i}$$

where $(\mathrm{COV})_i$ is the coefficient of variation of layer $i$ in percentage; $(D_\mathrm{F})_i$ is the depth factor that varies linearly from a value of 1 at ground surface to 0 at a depth of 20 m; $(T_\mathrm{N})_i$ is the normalized thickness of layer $i$ with respect to a nominal thickness of 20 m; and $(R_\Gamma)_i$ is a factor that depends on the type of correlation structure and the spatial range.

The factor $R_\Gamma$ was obtained through regression analysis of the relation between the square root of the variance reduction factor ($\Gamma$) and the ratio between the average layer thickness and the spatial range ($T_{av}/a$), as shown in Fig. 20 for exponential variograms. The results of the regression analysis can be expressed in the form

$$[19a]\quad R_\Gamma = 1 - 0.25\left(\frac{T_{av}}{a/3}\right) \qquad \text{for spherical variograms}$$

$$[19b]\quad R_\Gamma = 1 - 0.15\left(\frac{T_{av}}{a/3}\right) + 0.015\left(\frac{T_{av}}{a/3}\right)^2 \qquad \text{for exponential variograms}$$

The value of OVF was found to be 5.49 for the Wildlife Site. Sites with greater OVF values will be expected to exhibit higher variability than those considered in this study.

## Conclusions

The effect of ground heterogeneity on earthquake-induced ground response at the Wildlife Site was investigated in this study. This was carried out through the assessment of different ground lithologies and by applying geostatistical principles to estimate elements of soil inherent spatial variability using the results of 11 cone penetration tests conducted at the site covering an area of about 800 m$^2$. The CPT results were used stochastically, using Monte Carlo simulation techniques, to estimate the factor of safety against liquefaction and to examine different damage criteria, such as total liquefaction damage, $P_\mathrm{L}$, and liquefaction-induced surface settlement.

The use of mean values in CPT liquefaction analysis was found to be on the unsafe side. This was indicated by the analysis of ground response during the Westmoreland earthquake, where mean factors of safety were found to be greater than one for different potentially liquefiable layers at the site even though liquefaction was observed. This could be attributed to the fact that using mean values in liquefaction assessment cannot capture the presence of looser pockets within the soil mass. Moreover, it was found that depending on safety factors solely might not be an accurate measure of liquefaction susceptibility, as it does not necessarily capture the effect of embedment depth on the liquefaction potential of the site. As a result, an equivalent failure probability was proposed to take into consideration the effect of embedment depth and the thickness of different

**Fig. 15.** A site plan showing contours of probability of liquefaction-induced settlements greater than 10 cm for the Westmoreland earthquake.

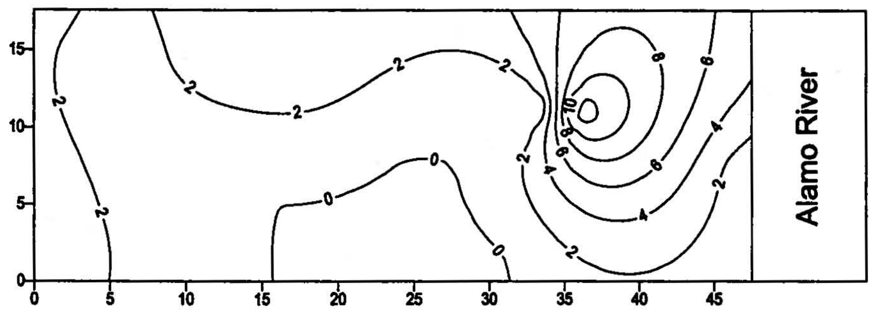


**Fig. 16.** A site plan showing the effective statistical area ($A_1$).

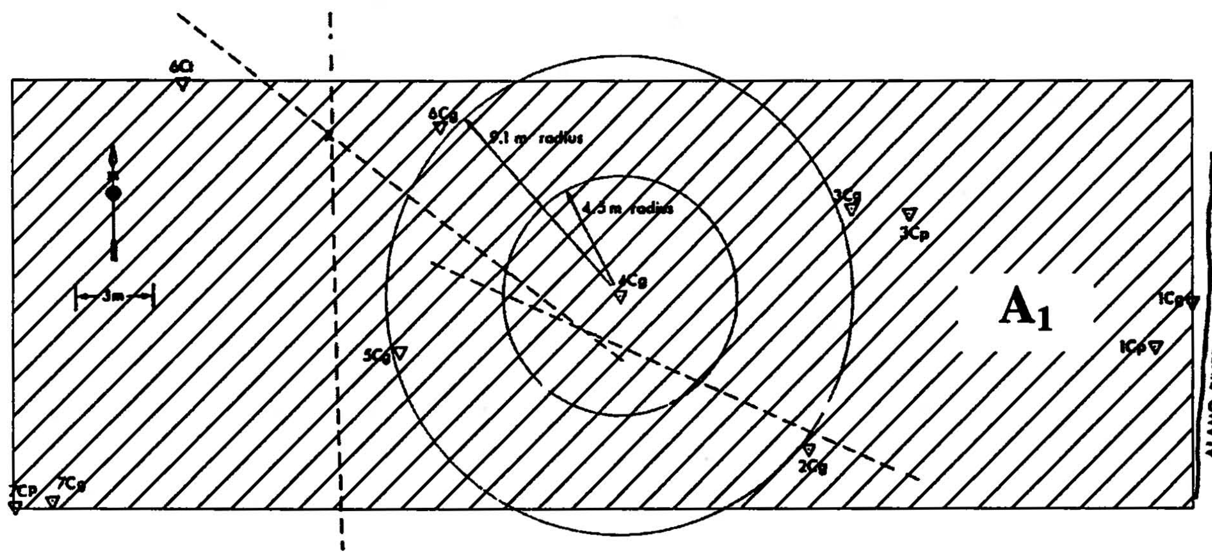


**Fig. 17.** Determination of a characteristic percentile of cone tip resistance associated with the liquefaction assessment at the Wildlife Site.

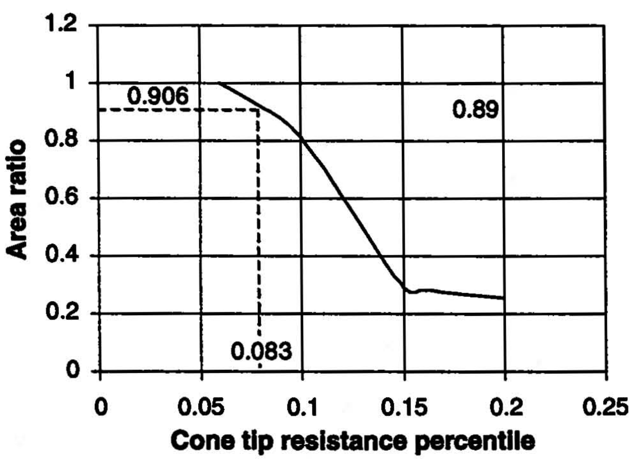


**Fig. 18.** Determination of a characteristic percentile of cone tips resistance associated with liquefaction-induced settlement at the Wildlife Site under the effect of the 1987 Superstition Hill earthquake.

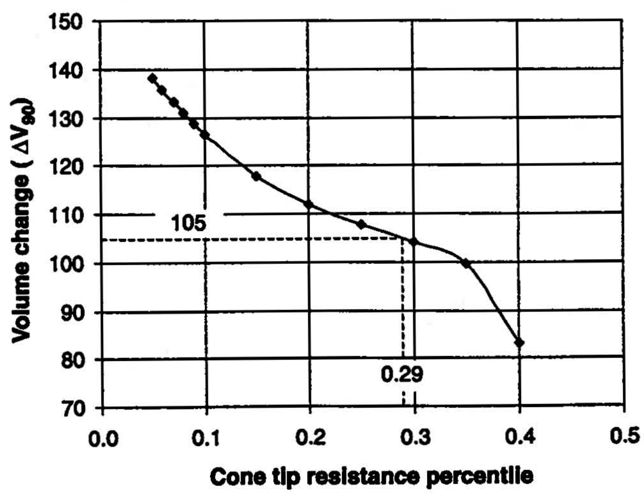


liquefiable layers. An equivalent failure probability of 1.2 to 15% was assessed as a critical threshold above which liquefaction would likely occur.

It was found that zones of surface damage were likely to be associated with a 1.2% probability, or higher, that total liquefaction damage, $P_L$, would exceed 5. In a similar fashion, these zones were found to be correlated with a 12% probability, or higher, that liquefaction-induced settlement would be greater than 10 cm. In addition, settlement profiles associated with the upper and lower limits of the 90% confi-

**Fig. 19.** A site plan of the effective statistical area at the Wildlife Site showing the influence area of each CPT sounding used to calculate the overall variability factor (OVF).

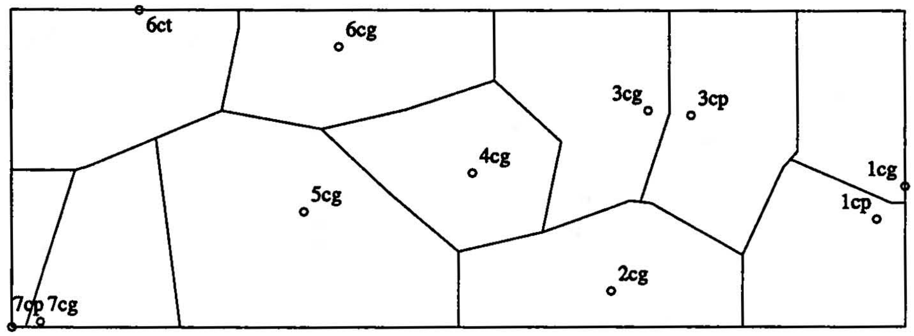


**Fig. 20.** The regression analysis used to obtain the factor $R_\Gamma$ for exponential variograms.

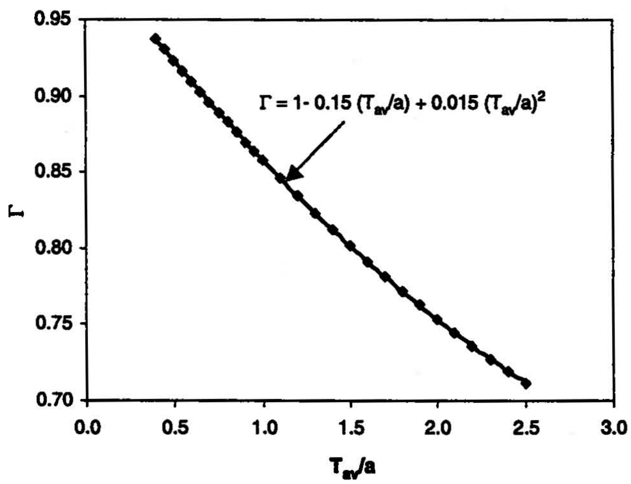


dence interval were introduced to account for the effect of ground variability on liquefaction settlement analyses. Using this interval in engineering design provides risk-based estimates of expected settlement at potentially liquefiable sites with a chance of only 5% that the actual settlement will be greater/smaller than the upper/lower limit.

Equivalent representative soil parameters were obtained for use in simplified deterministic analysis to assess liquefaction susceptibility and maximum ground settlement. It was concluded that liquefaction would not likely occur if no settlement greater than 10 cm was predicted anywhere across the site upon the use of a percentile of $q_c$ = 0.085 in deterministic settlement analyses. The 0.085 percentile can be defined as the value of cone tip resistance below which 8.5% of $q_c$ data occur. More efforts are needed to obtain characteristic percentiles for liquefaction-induced settlement prediction as these percentiles were found to be dependent on the shear stress generated in the ground during earthquake excitation. However, a range of characteristic percentiles between 0.17 and 0.29 was obtained in this study based on the upper limit of the 90% confidence interval. In other words, using this range in a simplified deterministic analysis implies that there will be only a 5% chance that the actual ground settlements will be greater than the predicted values.

It should be emphasized that the results obtained in this study are valid for sites with similar subsurface conditions and geostatistical characteristics, and they need to be verified and refined by analyzing more case histories and earthquake excitations. However, they can be used as relatively conservative measures for sites of smaller ground variability. To compare the degree of variability of different potentially liquefiable sites, an empirical factor, the overall variability factor (OVF), was developed in this study. The higher the value of OVF, the greater the ground variability expected at the site. In addition, it should be realized that the outcomes of this study were obtained using specific analysis techniques, such as the CSR–CRR for liquefaction assessment, Iwasaki's method for quantification of liquefaction damage, and Ishihara's method for estimation of liquefaction-induced surface damage. Each of these analysis techniques has its own inherent uncertainty that might affect the outcome of geostatistical liquefaction analyses. The assessment of such uncertainty was considered to be beyond the scope of this simplified study. As a result, the outcome of this study should not be extended to other case histories where different analysis methods are used.

It is worth noting that more efforts are needed to quantify the effect of other sources of uncertainty, which were not considered in this study, on the outcome of stochastic analyses of liquefaction case histories. These uncertainties can be summarized as follows:

(1) uncertainty resulting from spatial variation of CPT sleeve friction;

(2) uncertainty associated with selecting vertical trends of field data to fulfill stationarity requirements;

(3) uncertainty in selecting upper and lower boundaries of potentially liquefiable layers;

(4) uncertainty in estimating variogram characteristics due to the coordinates transformation process and selecting a theoretical model that best fits the field data variogram; and

(5) inherent uncertainty in the equations used in the assessment of liquefaction susceptibility and liquefaction-induced damage and settlement, such as the CSR–CRR approach, Iwasaki's damage criterion, and Ishihara's settlement curves.

Additional attention should be given to the site investigation process to provide sufficient field data to reliably assess different elements of soil spatial variability. Finally, there is a need to develop a generic decision making process for different geotechnical field problems depending on the risk level associated with these problems.

## References

Ambraseys, N.N. 1988. Engineering seismology. Earthquake Engineering and Structural Dynamics, **17**: 1–105.

Baziar, M., Dobry, R., and Alemi, M. 1992. Evaluation of lateral ground deformation using sliding block model. *In* Proceedings of the 10th world conference on earthquake engineering. Madrid, Spain, Vol. 3, pp. 1401–1406

Beaty, M., and Byrne, P. 1998. An effective stress model for predicting liquefaction behavior of sand. *In* Geotechnical Earthquake Engineering and Soil Dynamics III. Geotechnical Special Publication No. 75, Vol. 1, pp. 766–777.

Bennett, M.J., Mclaughlin, P.V., Sarmiento, J.S., and Youd, T.L. 1984. Geotechnical investigation of liquefaction sites, Imperial valley, California. Open-file Report 84–252, U.S. Geological Survey, Washington D.C.

Campanella, R.G., Wickremesinghe, D.S., and Robertson, P.K. 1987. Statistical treatment of cone penetration test data. Reliability and Risk Analysis in Civil Engineering. *In* Proceedings of ICAPS 5, the 5th International Conference on Applications of Statistics and Probability in Soil and Structural Engineering. Vancouver, B.C., Canada, pp. 1011–1019.

Deutsch, C.V. 2002. Geostatistical reservoir modeling. Oxford University Press, Oxford, New York.

Deutsch, C.V., and Journel, A.G. 1998. GSLIB geostatistical software library. Oxford University Press, Oxford, New York.

Dobry, R. 1994. Foundation deformation due to earthquakes. *In* Proceedings of the Conference on Vertical and Horizontal Deformations of Foundations and Embankment, College Station, Texas, U.S.A. Geotechnical Special Publications No. 40, Vol. 2, pp. 1846–1863.

Dobry, R., Elgamal, A., Baziar, M., and Vucetic, M. 1989. Pore pressure and acceleration response of Wildlife Site during the 1987 earthquake. *In* Proceedings of the 2nd U.S-Japan Workshop on Liquefaction, Large Deformation and Effect on buried Pipelines. Niagara Falls, NY, U.S.A., pp. 145–160.

Elkateb, T., Chalaturnyk, R., and Robertson, P.K. 2002. Quantification of soil heterogeneity and its implications on geotechnical field problems. Paper submitted to the Canadian Geotechnical Journal.

Fenton, G.A., and Vanmarcke, E.H. 1991. Spatial variation in liquefaction risk assessment. *In* Proceedings of the Geotechnical Engineering Congress, Boulder, Colorado, U.S.A. Geotechnical Special Publications No. 27, Vol. 1, pp. 594–607.

Gu, W.H., Morgenstern, N.R., and Robertson, P.K. 1994. Post-earthquake deformation analysis of Wildlife Site. Journal of the Geotechnical Engineering Division, ASCE, 120 GT(2): 274–289.

Harder, H., and Von Bloh, G. 1988. Determination of representative CPT-parameters. *In* Penetration testing in the U.K., Thomas Telford, London, pp. 237–240.

Idriss, I.M. 1995. The 1995 Seed Memorial Lecture, University of California at Berkeley (I.M. Idriss, personal communication to T.L. Youd, 1997).

Ishihara, K. 1993. Liquefaction and flow failure during earthquakes. The 33rd Rankin Lecture. Geotechnique, **43**(3): 351–415.

Ishihara, K., and Yoshimine, M. 1992. Evaluation of settlements in sand deposits following liquefaction during earthquakes. Soils and Foundations, **32**(1): 178–188.

Itasca Consulting Group. 1993. FLAC Fast Lagrangian Analysis of Continua. Program Software Version 3.22, Minneapolis, Minnesota.

Iwasaki, T., Tatsuoka, F., Tokida, F., and Yasuda, S. 1978. A practical method for assessing soil liquefaction potential based on case studies at various sites in Japan. *In* Proceedings of the Second Conference on Microzonation. San Francisco, CA, U.S.A., Vol. 2, pp. 885–896.

Krinitzsky, E.L., Chang, F.K., and Nuttli, O.W. 1988. Magnitude-related earthquake ground motions. Bulletin of the Association of Engineering Geologists, **25**(4): 399–423.

O'Rourke, T., and Hamada, M. 1992. *In* Case studies of liquefaction and lifeline performance during past earthquakes. Vol. 2, United States Case Studies. Technical Report NCEER-92–0002

Palisade Corporation. 1996. @Risk: Risk analysis and simulation add-in for Microsoft Excel or Lotus 1–2–3. Palisade Corporation, NY, U.S.A.

Popescu, R., Prevost, J.H., and Deodatis, G. 1998. Characteristic percentile of soil strength for dynamic analysis. *In* Proceedings of the 1998 Conference on Geotechnical Earthquake Engineering and Soil Dynamics III. Vol. 2, Seattle, WA, U.S.A., pp. 1461–1471.

Robertson, P.K. 1990. Soil classification using the cone penetration test. Canadian Geotechnical Journal, **27**(1): 151–158.

Robertson, P.K., and Wride, C.E. 1998. Evaluating cyclic liquefaction potential using the cone penetration test. Canadian Geotechnical Journal, **35**(3): 442–459

Seed, H.B., and Idriss, I.M. 1971. Simplified procedure for evaluating soil liquefaction potential. Journal of Soil Mechanics and Foundation Division, ASCE, 97 (SM9): 1249–1273

Vanmarcke, E. 1977. Probabilistic modeling of soil profiles. Journal of the Geotechnical Engineering Division, ASCE, 103 GT(11): 1227–1245.

Vanmarcke, E.H. 1984. Random fields, analysis and synthesis. MIT Press, Cambridge, MA.

Youd, T.L., Idriss, I.M., Andrus, R.D., Arango, I., Castro, G., Christian, J.T., Dobry, R., Finn, W.D.L., Harder Jr., L.F., Hynes, M.E., Ishihara, K., Koester, J.P., Liao S.S.C., Marcuson III, W.F., Martin, G.R., Mitchell, J.K., Moriwaki, Y., Power, M.S., Robertson, P.K., Seed, R.B., and Stokoe II, K.H. 2001. Liquefaction Resistance of Soils: Summary Report from the 1996 NCEER and 1998 NCEER/NSF Workshops on Evaluation of Liquefaction Resistance of Soils. Journal of the Geotechnical Engineering Division, ASCE, 127 GT(10): 817–833.

Zeghal, M., and Elgamal, A. 1994. Analysis of site liquefaction using Earthquake records. Journal of the Geotechnical Engineering Division, ASCE, 120 GT(6): 996–1017.

## Appendix A

### Liquefaction-induced ground settlement at different cpt locations

A summary of the main statistical characteristics of ground settlement at the Wildlife Site can be found in Table A1 as outlined below.

**Table A1.** Statistical characteristics of liquefaction-induced ground settlement at the Wildlife Site.

| Profile | $m$ (cm) | $\sigma$ (cm) | $P_{10}$ (%) | $S_5$ (cm) | $S_{95}$ (cm) |
|---|---|---|---|---|---|
| **Superstition Hill earthquake (1987)** | | | | | |
| 1cg | 7.835 | 2.188 | 16.96 | 4.600 | 11.700 |
| 1cp | 9.153 | 2.298 | 32.42 | 5.400 | 12.988 |
| 3cp | 13.262 | 2.489 | 90.55 | 9.028 | 17.158 |
| 3cg | 7.610 | 1.628 | 6.56 | 4.812 | 10.040 |
| 2cg | 7.758 | 4.099 | 26.71 | 3.000 | 15.644 |
| 4cg | 6.039 | 2.615 | 11.09 | 2.751 | 10.930 |
| 6cg | 10.385 | 1.979 | 59.25 | 6.949 | 13.340 |
| 5cg | 6.900 | 2.772 | 18.39 | 3.382 | 12.150 |
| 6ct | 7.055 | 4.429 | 27.28 | 0.662 | 14.720 |
| 7cg | 6.369 | 5.362 | 25.91 | 0.183 | 16.690 |
| 7cp | 4.454 | 3.826 | 13.52 | 0.113 | 11.983 |
| **Elmore Ranch earthquake (1987)** | | | | | |
| 1cg | 0.702 | 0.579 | <0.01 | 0.010 | 1.750 |
| 1cp | 0.797 | 0.630 | <0.01 | 0.010 | 1.920 |
| 3cp | 1.084 | 0.730 | <0.01 | 0.070 | 2.420 |
| 3cg | 0.701 | 0.602 | <0.01 | 0.004 | 1.850 |
| 2cg | 0.565 | 0.489 | <0.01 | 0.005 | 1.530 |
| 4cg | 0.469 | 0.414 | <0.01 | 0.004 | 1.290 |
| 6cg | 0.889 | 0.669 | <0.01 | 0.031 | 2.100 |
| 5cg | 0.553 | 0.480 | <0.01 | 0.005 | 1.510 |
| 6ct | 0.402 | 0.357 | <0.01 | 0.006 | 1.100 |
| 7cg | 0.222 | 0.338 | <0.01 | 0.000 | 1.130 |
| 7cp | 0.181 | 0.281 | <0.01 | 0.000 | 0.960 |
| **Westmoreland earthquake (1981)** | | | | | |
| 1cg | 3.888 | 1.966 | 0.620 | 0.720 | 7.200 |
| 1cp | 4.582 | 2.240 | 1.780 | 0.910 | 8.310 |
| 3cp | 6.732 | 3.041 | 13.260 | 1.650 | 11.800 |
| 3cg | 3.879 | 1.884 | 0.340 | 0.800 | 7.130 |
| 2cg | 2.989 | 1.613 | 0.110 | 0.430 | 5.690 |
| 4cg | 2.463 | 1.411 | 0.030 | 0.270 | 4.860 |
| 6cg | 5.298 | 2.461 | 3.900 | 1.2170 | 9.440 |
| 5cg | 2.938 | 1.566 | 0.090 | 0.380 | 5.480 |
| 6ct | 2.370 | 2.288 | 1.710 | 0.021 | 6.840 |
| 7cg | 1.544 | 2.288 | 2.760 | 0.000 | 4.690 |
| 7cp | 1.290 | 2.099 | 2.380 | 0.000 | 5.650 |
| **1979 Earthquake** | | | | | |
| 1cg | 0.865 | 0.700 | <0.01 | 0.020 | 2.250 |
| 1cp | 0.983 | 0.775 | <0.01 | 0.030 | 2.490 |
| 3cp | 1.332 | 0.913 | <0.01 | 0.100 | 3.040 |
| 3cg | 0.863 | 0.724 | <0.01 | 0.020 | 2.300 |
| 2cg | 0.697 | 0.576 | <0.01 | 0.015 | 1.810 |
| 4cg | 0.577 | 0.484 | <0.01 | 0.013 | 1.520 |
| 6cg | 1.096 | 0.832 | <0.01 | 0.050 | 2.680 |
| 5cg | 0.680 | 0.564 | <0.01 | 0.016 | 1.790 |
| 6ct | 0.499 | 0.422 | <0.01 | 0.009 | 1.310 |
| 7cg | 0.287 | 0.409 | <0.01 | 0.000 | 1.380 |

**Note:** $P_{10}$ is the probability of occurrence of settlement greater than 10 cm; $S_5$ is the settlement associated with the lower limit of 90% confidence interval; $S_{95}$ is the settlement associated with the upper limit of 90% confidence interval.